symmetry MDPI

*Article*

# Vacuum Currents for a Scalar Field in Models with Compact Dimensions

**Aram A. Saharian**

Institute of Physics, Yerevan State University, 1 Alex Manogian Street, Yerevan 0025, Armenia; saharian@ysu.am

**Abstract:** This paper presents a review of investigations into the vacuum expectation value of the current density for a charged scalar field in spacetimes that hold toroidally compactified spatial dimensions. As background geometries, the locally Minkowskian (LM), locally de Sitter (LdS), and locally anti-de Sitter (LAdS) spacetimes are considered. Along compact dimensions, quasi-periodicity conditions are imposed on the field operator and the presence of a constant gauge field is assumed. The vacuum current has nonzero components along the compact dimensions only. Those components are periodic functions of the magnetic flux enclosed in compact dimensions, with a period that is equal to the flux quantum. For LdS and LAdS geometries, and for small values of the length of a compact dimension, compared with the curvature radius, the leading term in the expansion of the the vacuum current along that dimension coincides with that for LM bulk. In this limit, the dominant contribution to the mode sum for the current density comes from the vacuum fluctuations with wavelengths smaller to those of the curvature radius; additionally, the influence of the gravitational field is weak. The effects of the gravitational field are essential for lengths of compact dimensions that are larger than the curvature radius. In particular, instead of the exponential suppression of the current density in LM bulk, one can obtain a power law decay in the LdS and LAdS spacetimes.

**Keywords:** vacuum currents; nontrivial topology; Casimir effect; de Sitter spacetime; anti-de Sitter spacetime

check for updates

**Citation:** Saharian, A.A. Vacuum Currents for a Scalar Field in Models with Compact Dimensions. *Symmetry* **2024**, *16*, 92. https://doi.org/10.3390/sym16010092

Academic Editors: Olga Kodolova, Tomohiro Inagaki and Alberto Ruiz Jimeno

Received: 13 December 2023
Revised: 6 January 2024
Accepted: 8 January 2024
Published: 11 January 2024



## 1. Introduction

In a number of physical models, the dynamics of the system are formulated in background geometries that have compact dimensions. The examples include Kaluza–Klein type models with extra dimensions, string theories with different types of compactifications of six-dimensional internal sub-spaces, condensed matter systems like fullerenes, cylindrical nanotubes and toroidal loops. The periodicity conditions imposed on dynamical variables along compact dimensions are sources of a number of interesting effects, such as the topological generation of mass, various mechanisms for symmetry breaking, and different kinds of instabilities (see, for example, [1–9]). In quantum field theory, nontrivial spatial topology modifies the spectrum of the zero-point fluctuations of the fields; as a consequence, the vacuum expectation values (VEVs) of physical observables are shifted by an amount that depends on the geometrical characteristics of the compact space. This is the analog of the Casimir effect (for reviews see [10–14]), where the conditions imposed on constraining boundaries are replaced by periodicity conditions; this is generally known as the topological Casimir effect. In Kaluza–Klein models, this effect yields an effective potential for the lengths of compact dimensions and can serve as a compactification and stabilization mechanism for internal sub-spaces (the Candelas–Weinberg mechanism [15]).

The most popular quantity in the investigations of the zero-temperature Casimir effect is that of vacuum energy. This is an important global characteristic of the vacuum state; additionally, it determines the vacuum forces that act onthe boundaries that constrain the quantization volume. More detailed information is contained in local characteristics, such as the vacuum expectation value (VEV) of the energy–momentum tensor. The latter is a source of the gravitational field in semi-classical Einstein equations and determines the back-reaction of the quantum effects on the geometry of the spacetime. That VEV of the energy–momentum tensor in the Casimir effect does not generally obey the energy conditions in Hawking–Penrose singularity theorems; hence, it is an interesting source of singularity-free solutions for the gravitational field. For charged fields, another important local characteristic of the vacuum state is the expectation value of the current density. It is a source of the electromagnetic field in Maxwell equations and should be taken into account when considering the self-consistent dynamics of the electromagnetic field.

Unlike the energy–momentum tensor, in order to achieve nonzero vacuum currents, the parity symmetry of the model should be broken. This can be performed by introducing external fields or by imposing appropriate boundary or periodicity conditions (in models with compact spatial dimensions). In particular, the vacuum currents for charged scalar and fermionic fields in locally Minkowski spacetime with toroidally compactified spatial dimensions and in the presence of constant gauge fields have been investigated in [16,17]. The parity symmetry in the corresponding models is broken by an external gauge field or by quasi-periodic conditions along compact dimensions with nontrivial phases. The results for a fermionic field in (2 + 1)-dimensional spacetime have been applied to carbon nanotubes and nanoloops. Those structures are obtained from planar graphene sheets through appropriate identifications along single or double spatial dimensions. In the long wavelength approximation, the dynamics of the electronic subsystems in graphene are well described through an effective Dirac model; here, the Fermi velocity of electrons appears instead of the velocity of light (see, for example, [18,19]). The corresponding quantum field theory lives in spaces with the $R^1 \times S^1$ and $S^1 \times S^1$ topologies for nanotubes and nanoloops, respectively. The appearance of the vacuum currents along compact dimensions can be understood as a kind of topological Casimir effect. The combined influence of the boundary-induced and topological Casimir effects on the vacuum currents have been studied in [20,21] for scalar and fermionic fields in the context of locally flat spacetime with toral dimensions, while in the presence of planar boundaries.

The boundary conditions imposed on quantum fields serve as simplified models for external fields; the Casimir effect can be considered to be a vacuum polarization that is sourced by those conditions. Another type of vacuum polarization can be induced by external gravitational fields. The combined effects of those two sources on the VEV of the current density have been investigated in [22–24] for locally de Sitter (dS) and anti-de Sitter (AdS) spacetimes with a part of the spatial dimensions compactified to a torus. The high symmetry of these background geometries permits the discovery of exact expressions for current densities in scalar and fermionic vacua. The effects of additional boundaries that are parallel to the AdS boundary were studied in [25–28]. The corresponding applications to higher-dimensional braneworld models with compact sub-spaces have been discussed.

The physical nature of the current densities considered in [16,17] is similar to that for persistent currents in mesoscopic rings [29–34]. Those currents are among the most interesting manifestations of the Aharonov–Bohm effect and appear as a result of phase coherence of the charge carriers, extended over the whole mesoscopic ring. The persistent currents have been studied extensively in the literature for electronic subsystems in different condensed matter systems and for bosonic and fermionic atoms by making use of discrete or continuum models (see, for example, [35–59] for theoretical and experimental investigations, respectively, and the references therein). Their dependence on the geometry of ring is an interesting direction of those investigations.

The present paper reviews the results of investigations of the vacuum current densities for charged scalar fields in locally Minkowski, dS and AdS spacetimes with toroidal sub-spaces. The paper is organized as follows. In Section 2, we present the general approach that was taken in our evaluation of the current densities for a charged scalar-filled model with compact dimensions. The application of the formalism in the locally Minkowskian background geometry is considered in Section 3. The vacuum currents for locally dS and AdS background spacetimes are studied in Sections 4 and 5. The features of current densities and the comparative analysis for the background geometries with zero, positive, and negative curvatures are discussed in Section 6. The main results are summarized in Section 7. In Appendix A, we present the properties of the functions appearing in the expressions of the current densities.

## 2. General Formalism

Consider a charged scalar field $\varphi(x)$ with the curvature coupling parameter $\xi$, in the background of $(D+1)$-dimensional spacetime, as described by the line element $ds^2 = g_{\mu\nu}(x)dx^\mu dx^\nu$. Here, we use $x = (x^0 = t, x^1, \dots, x^D)$ for the notation of the spacetime points. In the presence of a classical vector gauge field, $A_\mu(x)$, the corresponding action has the form

$$S[\varphi] = \frac{1}{2}\int d^{D+1}x\,\sqrt{|g|}\Big[g^{\mu\nu}(D_\mu\varphi)(D_\nu\varphi)^\dagger + \Big(\xi R + m^2\Big)\varphi\varphi^\dagger\Big]. \tag{1}$$

where $R$ is the Ricci scalar for the metric tensor $g_{\mu\nu}(x)$ and $D_\mu = \nabla_\mu + ieA_\mu$, with $\nabla_\mu$ being the related covariant derivative operator. The most important special cases correspond to the fields with minimal ($\xi = 0$) and conformal ($\xi = \xi_D \equiv (D-1)/(4D)$) couplings. The field equation obtained from (1) through the standard variational procedure reads

$$\Big(g^{\mu\nu}D_\mu D_\nu + \xi R + m^2\Big)\varphi(x) = 0. \tag{2}$$

We assume that a part of the coordinates corresponding to the sub-space $(x^{p+1}, x^{p+2}, \dots, x^D)$ are compactified to circles of the lengths $(L_{p+1}, L_{p+2}, \dots, L_D)$, respectively, and $0 \le x^l \le L_l$, $l = p+1, \dots, D$. In addition, the metric tensor is periodic along the following compact dimensions:

$$g_{\mu\nu}(t, x^1, \dots, x^p, \dots, x^l + L_l, \dots, x^D) = g_{\mu\nu}(t, x^1, \dots, x^p, \dots, x^l, \dots, x^D), \tag{3}$$

where $p < l \le D$. For the scalar and gauge fields, less trivial quasi-periodicity conditions are imposed.

$$\begin{aligned}\varphi(t, x^1, \dots, x^p, \dots, x^l + L_l, \dots, x^D) &= e^{i\alpha_l(x)}\varphi(t, x^1, \dots, x^p, \dots, x^l, \dots, x^D),\\ A_\mu(t, x^1, \dots, x^p, \dots, x^l + L_l, \dots, x^D) &= A_\mu(t, x^1, \dots, x^p, \dots, x^l, \dots, x^D) - (1/e)\nabla_\mu\alpha_l(x),\end{aligned} \tag{4}$$

where the real functions, $\alpha_l(x)$, $l = p+1, \dots, D$, are periodic along the compact dimensions. With these conditions, the Lagrangian density in (1) is periodic in the subspace $(x^{p+1}, x^{p+2}, \dots, x^D)$. The gauge field is periodic up to a gauge transformation, and these types of quasi-periodic conditions are referred as C-periodic boundary conditions (see, for example, [60–62]).

We are interested in the VEV of the current density

$$j_\mu = \frac{i}{2}e\Big[\{D_\mu\varphi, \varphi^\dagger\} - \{D_\mu\varphi, \varphi^\dagger\}^\dagger\Big], \tag{5}$$

where the figure brackets stand for the anti-commutator. The VEVs of the field bilinear combinations are expressed in terms of the Hadamard function, $G(x, x')$, defined as the VEV

$$G(x, x') = \Big\langle\{\varphi(x), \varphi^\dagger(x')\}\Big\rangle, \tag{6}$$

where $\langle\cdots\rangle = \langle 0|\cdots|0\rangle$—with $|0\rangle$ being the vacuum state—stands for the VEV. In particular, for the VEV of the current density, we have

$$\langle j_\mu(x)\rangle = \frac{ie}{2}\lim_{x'\to x}\Big(D_\mu - g_\mu{}^{\nu'}D^*_{\nu'}\Big)G(x, x'), \tag{7}$$

with $g_{\mu}{}^{\nu'}$ being the bi-vector of the parallel displacement. We recall that the vector $\tilde{c}_{\mu} = g_{\mu}{}^{\nu'} c_{\nu'}$ is obtained using the parallel transport of $c_{\nu}$ from the point $x'$ to the point $x$ along the geodesic connecting those points.

The Hadamard function in (7) can be evaluated in two different ways: by solving the corresponding differential equation obtained from the field equation or by using the complete set $\{\varphi_{\sigma}^{(+)}(x), \varphi_{\sigma}^{(-)}(x)\}$ of the mode functions for the field specified by the set of quantum numbers $\sigma$. We will follow the second approach. For the field operator, one has the expansion

$$\varphi(x) = \sum_{\sigma}\Big[a_{\sigma}\varphi_{\sigma}^{(+)}(x) + b_{\sigma}^{\dagger}\varphi_{\sigma}^{(-)}(x)\Big], \tag{8}$$

where $a_{\sigma}$ and $b_{\sigma}^{\dagger}$ are the annihilation and creation operators. The symbol $\sum_{\sigma}$ stands for the summation over the discrete quantum numbers in the set $\sigma$ and the integration over the continuous ones. Substituting in the expression (6) for the Hadamard function and by using the relations $a_{\sigma}|0\rangle = b_{\sigma}|0\rangle = 0$, we obtain the mode sum

$$G(x, x') = \sum_{\sigma}\Big[\varphi_{\sigma}^{(+)}(x)\varphi_{\sigma}^{(+)*}(x') + \varphi_{\sigma}^{(-)}(x)\varphi_{\sigma}^{(-)*}(x')\Big]. \tag{9}$$

With this sum, the formal expression for the VEV of the current density takes the following form

$$\langle j_{\mu}\rangle = -e\sum_{\sigma}\mathrm{Im}\Big(\varphi_{\sigma}^{(+)*}D_{\mu}\varphi_{\sigma}^{(+)} + \varphi_{\sigma}^{(-)*}D_{\mu}\varphi_{\sigma}^{(-)}\Big). \tag{10}$$

The expression on the right-hand side is divergent; a regularization with the subsequent renormalization is required to obtain a finite result.

In the following sections, we apply the presented general formalism for special background geometries. Three cases will be considered: locally Minkowski spacetime (LM), locally dS spacetime (LdS), and locally AdS spacetime (LAdS). For all these geometries, the planar coordinates $\mathbf{x}_q = (x_{p+1}, \ldots, x_D)$ will be used in the compact sub-space. For the classical gauge field, we will assume a simple configuration $A_{\mu} = \mathrm{const}$ and, in the periodicity conditions (4), the phases $\alpha_l(x) = \alpha_l = \mathrm{const}$ will be taken. Special cases $\alpha_l = 2\pi$ and $\alpha_l = \pi$ correspond to the periodic and antiperiodic fields, respectively, and have been widely considered in the literature. The constant gauge field is removed from the field equation for the scalar field by the gauge transformation $(\varphi, A_{\mu}) \to \big(\varphi', A'_{\mu}\big)$, given as

$$\varphi'(x) = \varphi(x)e^{ie\chi(x)},\ A'_{\mu} = A_{\mu} - \partial_{\mu}\chi(x), \tag{11}$$

with the function $\chi(x) = A_{\mu}x^{\mu}$. For this function, one obtains $A'_{\mu} = 0$ and the field equation takes the form

$$\Big(g^{\mu\nu}\nabla_{\mu}\nabla_{\nu} + \xi R + m^2\Big)\varphi'(x) = 0. \tag{12}$$

The periodicity conditions for the new scalar field read

$$\varphi'(t, x^1, \ldots, x^p, \ldots, x^l + L_l, \ldots, x^D) = e^{i\tilde{\alpha}_l}\varphi'(t, x^1, \ldots, x^p, \ldots, x^l, \ldots, x^D), \tag{13}$$

with new phases

$$\tilde{\alpha}_l = \alpha_l + eA_lL_l, \tag{14}$$

for $l = p+1, \ldots, D$. The physics is invariant under the gauge transformation, and we could expect that the components $A_{\mu}$, $\mu = 0, 1, \ldots, p$, will not appear in the expressions for physical quantities. This is not the case for the components of the vector potential along the compact dimensions. They will appear in the VEVs through the new phases (14). This is an Aharonov–Bohm-type effect for a constant gauge field in topologically nontrivial spaces. The further consideration will be presented in terms of new fields, $\big(\varphi', A'_{\mu} = 0\big)$, omitting the primes.

## 3. Locally Minkowski Spacetime with Toral Dimensions

We start the consideration with LM spacetime having the spatial topology $R^p \times T^q$, $q = D - p$, where the $q$-dimensional torus $T^q$ corresponds to the sub-space with the compact coordinates $\mathbf{x}_q = (x^{p+1}, x^{p+2}, \ldots, x^D)$. For this geometry, the metric in the Cartesian coordinates is expressed as $g_{\mu\nu} = \eta_{\mu\nu} = \mathrm{diag}(1, -1, \ldots, -1)$. With this metric tensor, one has $\nabla_\mu = \partial_\mu$. The topological Casimir effect in flat spacetimes with toral dimensions has been widely considered in the literature (see [10,14,63–78] and references therein). As characteristics of the ground state for quantum fields, the expectation values of the energy density and the stresses were studied. The expectation value of the current density for scalar and fermionic fields have been investigated in [16,17,20,21,79] at zero and finite temperatures. In this section, we review the results for the VEV of the current density for a charged scalar field.

For the geometry under consideration, the normalized scalar mode functions are specified by the momentum $\mathbf{k} = (k_1, k_2, \ldots, k_D)$ and are given by

$$\varphi^{(\pm)}_{\mathbf{k}}(x) = (2^{p+1}\pi^p V_q \omega_{\mathbf{k}})^{-1/2} e^{\mp i\omega_{\mathbf{k}} t + \mathbf{k}_p\cdot\mathbf{x}_p + \mathbf{k}_q\cdot\mathbf{x}_q}, \tag{15}$$

where $\mathbf{x}_p = (x^1, \ldots, x^D)$ stands for the set of coordinates in the non-compact sub-space, $\omega_{\mathbf{k}} = \sqrt{\mathbf{k}^2 + m^2}$ is the respective energy, and $V_q = L_{p+1} \ldots L_D$. For the components of the momentum along non-compact dimensions, $\mathbf{k}_p = (k_1, \ldots, k_p)$, we have $k_l \in (-\infty, +\infty)$, $l = 1, \ldots, p$, whereas the eigenvalues along the compact dimensions, $\mathbf{k}_q = (k_{p+1}, \ldots, k_D)$, are discretized by the periodicity conditions (13):

$$k_l = \frac{2\pi n_l + \tilde{\alpha}_l}{L_l}, \quad n_l = 0, \pm 1, \pm 2, \ldots, \tag{16}$$

with $l = p+1, \ldots, D$. The integer part of the ratio $\tilde{\alpha}_l/(2\pi)$ in the expressions of the VEVs is absorbed by shifting the integer number $n_l$ in the corresponding summation and, hence, we can take $|\tilde{\alpha}_l| \le \pi$ without loss of generality. Note that one has

$$\varphi^{(\pm)}_{\mathbf{k}}(t, x^1, \ldots, x^p, \ldots, x^l - L_l, \ldots, x^D) = e^{-i\tilde{\alpha}_l}\varphi^{(\pm)}_{\mathbf{k}}(t, x^1, \ldots, x^p, \ldots, x^l, \ldots, x^D), \tag{17}$$

and hence for $\tilde{\alpha}_l \neq n\pi$, with $n$ being an integer, the parity (P-) symmetry with respect to the reflection $x^l \to -x^l$ is broken by the corresponding quasi-periodicity condition. As will be seen below, the breaking of this inversion symmetry results in a nonzero component of the current density along the $l$th compact dimension.

The Hadamard function is obtained from (9) with the modes (15). Because of the spacetime homogeneity the dependence on the coordinates appears in the form of differences $\Delta t = t - t'$, $\Delta\mathbf{x}_p = \mathbf{x}_p - \mathbf{x}'_p$, and $\Delta\mathbf{x}_q = \mathbf{x}_q - \mathbf{x}'_q$. Inserting the modes (15) in (9), one obtains

$$G(x, x') = \frac{1}{V_q}\int \frac{d\mathbf{k}_p}{(2\pi)^p} \sum_{\mathbf{n}_q} e^{i\mathbf{k}_p\cdot\Delta\mathbf{x}_p + i\mathbf{k}_q\cdot\Delta\mathbf{x}_q} \frac{\cos(\omega_{\mathbf{k}}\Delta t)}{\omega_{\mathbf{k}}}, \tag{18}$$

where $\mathbf{n}_q = (n_{p+1}, \ldots, n_D)$. In the gauge under consideration and for the geometry at hand, Formula (7) for the current density takes the form

$$\langle j_\mu \rangle = \frac{ie}{2} \lim_{x' \to x} \left(\partial_\mu - \partial_{\mu'}\right) G(x, x'). \tag{19}$$

For $\mu = 0, 1, \ldots, p$ the derivatives $\partial_\mu G(x, x')$ and $\partial_{\mu'} G(x, x')$ are odd functions of $\Delta x^\mu$ and the charge density and the components of the current density along the non-compact dimensions vanish, $\langle j_\mu \rangle = 0$ for $\mu = 0, 1, \ldots, p$. Of course, we could expect this outcome from the problem symmetry under the reflections $x^\mu \to -x^\mu$ along the respective coordinates. In order to find the current density along the $r$th compact dimension, it is convenient to transform the corresponding summation over $n_r$ in (18). In order to do that, we use a variant of the Abel–Plana formula [70,80]

$$\frac{2\pi}{L_r}\sum_{n_r=-\infty}^{\infty} g(k_r)f(|k_r|) = \sum_{\lambda=\pm 1}\left[\int_0^{\infty} dz g(\lambda z)f(z) + i\int_0^{\infty} dz\, g(i\lambda z)\frac{f(iz)-f(-iz)}{e^{zL_r+i\lambda\tilde{\alpha}_r}-1}\right], \quad (20)$$

with the functions $g(z) = e^{iz\Delta x^r}$ and $f(z) = \cos\left(\Delta t\sqrt{z^2+\omega_{p,q-1}^2}\right)/\sqrt{z^2+\omega_{p,q-1}^2}$, where $\omega_{p,q-1} = \sqrt{\mathbf{k}_p^2+\mathbf{k}_{q-1}^2+m^2}$ and $\mathbf{k}_{q-1} = (k_{p+1},\ldots,k_{r-1},k_{r+1},\ldots,k_D)$. By making use of the expansion $1/(e^y-1) = \sum_{l=1}^{\infty} e^{-ly}$, the integrals over $z$ and then over $\mathbf{k}_p$ are expressed in terms of the Macdonald function $K_\nu(x)$. Introducing the notation $f_\nu(x) = x^{-\nu}K_\nu(x)$, we obtain

$$G(x,x') = \frac{2L_rV_q^{-1}}{(2\pi)^{p/2+1}}\sum_{n_r=-\infty}^{+\infty}\sum_{\mathbf{n}_{q-1}} e^{in_r\tilde{\alpha}_r+i\mathbf{k}_{q-1}\cdot\Delta\mathbf{x}_{q-1}}\omega_{\mathbf{n}_{q-1}}^{p} f_{\frac{p}{2}}\left(\omega_{\mathbf{n}_{q-1}}\sqrt{|\Delta\mathbf{x}_p|^2+(\Delta x^r-n_rL_r)^2-(\Delta t)^2}\right), \quad (21)$$

where $\mathbf{n}_{q-1} = (n_{p+1},\ldots,n_{r-1},n_{r+1},\ldots,n_D)$ and $\omega_{\mathbf{n}_{q-1}}^2 = \mathbf{k}_{q-1}^2+m^2$. The $n_r=0$ term here corresponds to the Hadamard function in the geometry with spatial topology $R^{p+1}\times T^{q-1}$, where the $r$th dimension is decompactified. The divergences in the coincidence limit $x'\to x$ are contained in that term only. The remaining part is induced by the compactification of the coordinate $x^r$ and it is finite in the coincidence limit. The latter property is related to the fact that the compactification to a circle does not change the local geometry; hence, the structure of local divergences is also unchanged.

Plugging the Hadamard function (21) in (19) and noting that the term $n_r=0$ does not contribute to the component of the current density along the $r$th compact dimension, for the corresponding contravariant component, one finds

$$\langle j^r\rangle = \frac{2^{1-p/2}eL_r^2}{\pi^{p/2+1}V_q}\sum_{n_r=1}^{\infty} n_r\sin(n_r\tilde{\alpha}_r)\sum_{\mathbf{n}_{q-1}}\omega_{\mathbf{n}_{q-1}}^{p+2}f_{p/2+1}(n_rL_r\omega_{\mathbf{n}_{q-1}}). \quad (22)$$

The specific features of the vacuum current will be discussed below in Section 6. As has been already mentioned, for $\tilde{\alpha}_r = 0,\pi$ the problem is symmetric with respect to the inversion $x^r\to -x^r$ and, as expected, the VEV $\langle j^r\rangle$ vanishes. For those special values, the contribution from the right-moving vacuum fluctuations with $k_r>0$ is canceled by the contribution coming from the left-moving modes with $k_r<0$. For $\tilde{\alpha}_r=0$, there is also a zero mode with $k_r=0$; this does not contribute to the current density along the $r$th dimension.

In the model with a single compact dimension $x^D$, one has $p=D-1$, $\omega_{\mathbf{n}_{q-1}}=m$ and Formula (22) is reduced to

$$\left\langle j^D\right\rangle = \frac{4em^{D+1}L_D}{(2\pi)^{\frac{D+1}{2}}}\sum_{n=1}^{\infty} n\sin(n\tilde{\alpha}_D)f_{\frac{D+1}{2}}(mnL_D). \quad (23)$$

In particular, for a mass-less field, we obtain

$$\left\langle j^D\right\rangle = \frac{2e\Gamma\left(\frac{D+1}{2}\right)}{\pi^{\frac{D+1}{2}}L_D^D}\sum_{n=1}^{\infty}\frac{\sin(n\tilde{\alpha}_D)}{n^D}. \quad (24)$$

For odd values of $D$, the series is expressed in terms of the Bernoulli polynomials $B_n(x)$ (see, for example, [81]); we obtain

$$\left\langle j^D\right\rangle = \frac{(-1)^{\frac{D+1}{2}}\pi^{\frac{D}{2}}e}{\Gamma\left(\frac{D}{2}+1\right)L_D^D}B_D\left(\frac{\tilde{\alpha}_D}{2\pi}\right), \quad (25)$$

for $0 < \tilde{\alpha}_D < 2\pi$. In particular, for $D = 1$ and $D = 3$ one finds

$$\begin{aligned} \left\langle j^D \right\rangle &= \frac{e}{L_D}\left(1 - \frac{\tilde{\alpha}_D}{\pi}\right),\ D = 1, \\ \left\langle j^D \right\rangle &= \frac{e\tilde{\alpha}_D}{6L_D^3}\left(1 - \frac{\tilde{\alpha}_D}{\pi}\right)\left(2 - \frac{\tilde{\alpha}_D}{\pi}\right),\ D = 3. \end{aligned} \tag{26}$$

For $D \geq 2$, the current density is a continuous function of $\tilde{\alpha}_D$, whereas for $D = 1$, the current density for a mass-less field is discontinuous at $\tilde{\alpha}_D = 2\pi n$ with integer $n$.

We could directly start from the mode sum Formula (10) with $D_\mu = \partial_\mu$. The substitution of the mode functions (15) leads to the following expression

$$\langle j^r \rangle = \frac{e}{V_q}\int \frac{d\mathbf{k}_p}{(2\pi)^p}\sum_{\mathbf{n}_q}\frac{k_r}{\omega_{\mathbf{k}}} = \frac{eL_r}{V_q}\frac{\partial}{\partial\tilde{\alpha}_r}\int \frac{d\mathbf{k}_p}{(2\pi)^p}\sum_{\mathbf{n}_q}\omega_{\mathbf{k}}. \tag{27}$$

Introducing the generalized zeta function $\zeta(s)$ in accordance with

$$\zeta(s) = \frac{1}{V_q}\int \frac{d\mathbf{k}_p}{(2\pi)^p}\sum_{\mathbf{n}_q}\omega_{\mathbf{k}}^{-2s} = \frac{1}{V_q}\int \frac{d\mathbf{k}_p}{(2\pi)^p}\sum_{\mathbf{n}_q}\left(\mathbf{k}_p^2 + \mathbf{k}_q^2 + m^2\right)^{-s}, \tag{28}$$

the current density is written as

$$\langle j^r \rangle = eL_r \frac{\partial}{\partial\tilde{\alpha}_r}\zeta(s)\bigg|_{s=-1/2}, \tag{29}$$

where $|_{s=-1/2}$ is understood in the sense of the analytical continuation of the representation (28) (for applications of the zeta function technique in the investigations of the Casimir effect see, for example, [14,82,83]). In order to realize the analytic continuation, we first integrate over the momentum in the non-compact sub-space with the result

$$\zeta(s) = \frac{\Gamma(s - p/2)}{2^p\pi^{p/2}V_q\Gamma(s)}\sum_{\mathbf{n}_q}\left(\mathbf{k}_q^2 + m^2\right)^{p/2-s}. \tag{30}$$

The application of the generalized Chowla–Selberg Formula [84] to the multiple series in (30) gives

$$\zeta(s) = \frac{m^{D-2s}}{(4\pi)^{\frac{D}{2}}\Gamma(s)}\left[\Gamma\left(s - \frac{D}{2}\right) + 2^{\frac{D}{2}+1-s}\sum_{\mathbf{n}_q}{}'\cos\left(\mathbf{n}_q\cdot\tilde{\boldsymbol{\alpha}}_q\right)f_{\frac{D}{2}-s}(mg(\mathbf{L}_q, \mathbf{n}_q))\right], \tag{31}$$

where the prime on the summation sign means that the term with $\mathbf{n}_q = (0, 0, \ldots, 0)$ should be excluded. Here, we have introduced the $q$-component vector $\tilde{\boldsymbol{\alpha}}_q = (\tilde{\alpha}_{p+1}, \tilde{\alpha}_{p+2}, \ldots, \tilde{\alpha}_D)$ and the notation

$$g(\mathbf{L}_q, \mathbf{n}_q) = \left(\sum_{i=p+1}^{D} n_i^2 L_i^2\right)^{1/2}. \tag{32}$$

The first term in the right-hand side of (31) corresponds to the geometry without compact dimensions and it does not contribute to the current density. The last term in (31) is finite at the physical point and can be directly used in (29) to obtain the following expression for the current density:

$$\langle j^r \rangle = \frac{2em^{D+1}L_r}{(2\pi)^{\frac{D+1}{2}}}\sum_{\mathbf{n}_q}{}'n_r\sin\left(\mathbf{n}_q\cdot\tilde{\boldsymbol{\alpha}}_q\right)f_{\frac{D+1}{2}}(mg(\mathbf{L}_q, \mathbf{n}_q)). \tag{33}$$

In the special case of a single compact dimension $x^D$, this result coincides with (23). Note that, in the representation (33), we can make the replacement

$$n_r \sin\left(\mathbf{n}_q \cdot \tilde{\boldsymbol{\alpha}}_q\right) \rightarrow n_r \sin(n_r\tilde{\alpha}_r) \cos\left(\mathbf{n}_{q-1} \cdot \tilde{\boldsymbol{\alpha}}_{q-1}\right). \tag{34}$$

The representation with this replacement is given in [16]. The equivalence of two representations (22) and (33) follows from the relation

$$\sum_{\mathbf{n}_{q-1}} \left(z^2 + \mathbf{k}_{q-1}^2\right)^{\frac{s+1}{2}} f_{\frac{s+1}{2}}\left(n_r L_r \sqrt{z^2 + \mathbf{k}_{q-1}^2}\right) = \frac{V_q z^{s+q}}{(2\pi)^{\frac{q-1}{2}} L_r} \sum_{\mathbf{n}_{q-1}} \cos(\mathbf{n}_{q-1} \cdot \tilde{\boldsymbol{\alpha}}_{q-1}) f_{\frac{s+q}{2}}(z g(\mathbf{L}_q, \mathbf{n}_q)), \tag{35}$$

with $s = p + 1$ and $z = m$. This relation is proved in [70] by using the Poisson's resummation formula. For a mass-less field, by using the asymptotic for the modified Bessel function for small argument, one finds

$$\langle j^r \rangle = \frac{\Gamma\left(\frac{D+1}{2}\right)}{\pi^{\frac{D+1}{2}}} e L_r \sum_{\mathbf{n}_q}{}' \frac{n_r \sin\left(\mathbf{n}_q \cdot \tilde{\boldsymbol{\alpha}}_q\right)}{g^{D+1}\left(\mathbf{L}_q, \mathbf{n}_q\right)}. \tag{36}$$

For a single compact dimension, this formula coincides with (24). Properties of the current density described by (22) and (36) will be discussed in Section 6 below.

## 4. Current Density in Locally dS Spacetime with Compact Dimensions

In this section, we consider $(D+1)$-dimensional locally dS spacetime with a part of spatial dimensions compactified to $q$-dimensional torus in planar (inflationary) coordinates. It is the solution of the Einstein field equations with the positive cosmological constant $\Lambda$ as the only source of the $(D+1)$-dimensional gravitation. The standard dS spacetime (without compactification) is maximally symmetric and is one of the most popular background geometries in gravity and field theories. This has several motivations. First of all, the high degree of symmetry allows us to have a relatively large number of exactly solvable problems. The corresponding results shed light on the influence of the gravitational field on various physical processes in more complicated curved backgrounds. In accordance with the inflationary scenario, dS spacetime approximates the geometry of the early Universe and the investigation of the respective effects is an important step in understanding the dynamics of the Universe in the post-inflationary stage. In particular, the quantum fluctuations of the fields in the early dS phase of the expansion serve as seeds for large-scale structure formation in the Universe. This is currently the most popular mechanism for the formation of large-scale structures. Another motivation for the importance of dS spacetime is conditioned by its role in the $\Lambda$ CDM model for cosmological expansion. In that model, the accelerated expansion of the Universe at the recent epoch is sourced by a positive cosmological constant and dS spacetime appears as the future attractor of Universe expansion.

The explicit way to see the symmetries of the dS spacetime is in its embedding as a hyperboloid:

$$\left(Z^0\right)^2 - \left(Z^1\right)^2 - \cdots - \left(Z^{D+1}\right)^2 = -a^2, \tag{37}$$

in $(D+2)$-dimensional Minkowski spacetime with the line element $ds_{D+2}^{(\mathrm{M})2} = \left(dZ^0\right)^2 - \left(dZ^1\right)^2 - \cdots - \left(dZ^{D+1}\right)^2$. The parameter $a$ in (37) determines the curvature radius of dS spacetime. Different coordinate systems have been used to exclude an additional degree of freedom by using the relation (37). For the following discussion of the current density, we will use the planar coordinates $(\tau, x^1, x^2, \ldots, x^D)$ which are connected to the coordinates in the embedding spacetime by the following relations (see, for example, [85] in the case $D = 3$):

$$
\begin{aligned}
Z^i &= \frac{1}{2\tau}\left[a^2 + (-1)^i \left(\sum_{l=1}^{D}(x^l)^2 - \tau^2\right)\right],\ i = 0, 1, \\
Z^l &= \frac{a}{\tau}x^{l-1},\ l = 2, \dots, D+1.
\end{aligned} \tag{38}
$$

For the dS line element, this gives $ds^{(\mathrm{dS})2}_{D+1} = g_{\mu\nu}(x)dx^\mu dx^\nu$, with the metric tensor

$$
g_{\mu\nu}(x) = (a/\tau)^2\eta_{\mu\nu}. \tag{39}
$$

In inflationary models, a part of dS spacetime with the conformal time coordinate in the range $-\infty < \tau < 0$ is employed. For the corresponding synchronous time coordinate $t$, $-\infty < t < +\infty$, one has $t = -a\ln|\tau|/a$ and the line element is expressed as

$$
ds^{(\mathrm{dS})2}_{D+1} = dt^2 - \exp\left(\frac{2t}{\alpha}\right)\sum_{i=1}^{D}(dx^i)^2. \tag{40}
$$

The metric (39) is the solution of Einstein's equations with positive cosmological constant $\Lambda = \frac{D(D-1)}{2a^2}$ as the only source of the gravitational field.

The hyperbolic embedding (37) in the locally Minkowski spacetime with the line element $ds^{(\mathrm{M})2}_{D+2}$ works equally well for LdS spacetime with a $q$-dimensional toroidal sub-space covered by the coordinates $(x^{p+1}, x^{p+2}, \dots, x^D)$. The coordinate $x^l$, $l = p+1, \dots, D$, varies in the range $0 \le x^l \le L_l$. In this case, the sub-space with the coordinates $(Z^{p+2}, \dots, Z^{D+2})$ is compactified to a torus. The length of the compact dimension $Z^{l+1}$, $l = p+1, \dots, D$, is given by $L_{(\mathrm{p})l} = aL_l/\eta = e^{t/a}L_l$, with $\eta = |\tau|$. Note that $L_{(\mathrm{p})l}$ is the proper length of the compact dimension $x^l$ in the LdS spacetime.

For LdS spacetime with the metric tensor (39) and compact sub-space covered by the coordinates $\mathbf{x}_q = (x^{p+1}, x^{p+2}, \dots, x^D)$, the scalar mode functions can be presented in the form $\varphi^{(+)}_\sigma(x) = \eta^{D/2}g_\nu(k\eta)e^{i\mathbf{k}_p\cdot\mathbf{x}_p + i\mathbf{k}_q\cdot\mathbf{x}_q}$, where $g_\nu(y)$ is a cylinder function of the order

$$
\nu = \left[\frac{D^2}{4} - D(D+1)\xi - a^2m^2\right]^{1/2}. \tag{41}
$$

The eigenvalues of the momentum components along compact dimensions are given by (16). Different choices of the function $g_\nu(y)$ correspond to different vacuum states for a scalar field in dS spacetime. Here, we will investigate the current density in the Bunch–Davies vacuum state [86].

### 4.1. Hadamard Function

For the Bunch–Davies vacuum state, the normalized scalar mode functions are specified by $\sigma = \mathbf{k} = (\mathbf{k}_p, \mathbf{k}_q)$ and are expressed as

$$
\left\{\begin{array}{c} \varphi^{(+)}_{\mathbf{k}}(x) \\ \varphi^{(-)}_{\mathbf{k}}(x) \end{array}\right\} = \left(\frac{a^{1-D}e^{i(\nu-\nu^*)\pi/2}}{2^{p+2}\pi^{p-1}V_q}\right)^{\frac{1}{2}} e^{i\mathbf{k}_p\cdot\mathbf{x}_p + i\mathbf{k}_q\cdot\mathbf{x}_q}\eta^{D/2}\left\{\begin{array}{c} H^{(1)}_\nu(k\eta) \\ H^{(2)}_{\nu^*}(k\eta) \end{array}\right\}, \tag{42}
$$

where $H^{(1,2)}_\nu(y)$ are the Hankel functions and the star stands for the complex conjugate. Note that, depending on the curvature coupling parameter and on the mass of the field quanta, the order of the Hankel functions can be either non-negative real or purely imaginary. With the modes (42), the mode sum for the Hadamard function reads

$$
G(x,x') = \frac{(\eta\eta')^{\frac{D}{2}}e^{i\frac{\pi}{2}(\nu-\nu^*)}}{2^{p+2}\pi^{p-1}V_q a^{D-1}}\int d\mathbf{k}_p \sum_{\mathbf{n}_q} e^{i\mathbf{k}_p\cdot\Delta\mathbf{x}_p + i\mathbf{k}_q\cdot\Delta\mathbf{x}_q}[H^{(1)}_\nu(k\eta)H^{(2)}_{\nu^*}(k\eta') + H^{(1)}_\nu(k\eta')H^{(2)}_{\nu^*}(k\eta)]. \tag{43}
$$

Applying to the sum over $n_r$ the summation Formula (20) and assuming that $\mathrm{Re}\,\nu < 1$, one finds the representation

$$\begin{aligned} G(x,x') &= \frac{4(\eta\eta')^{\frac{D}{2}} L_r}{(2\pi)^{\frac{p+3}{2}} V_q a^{D-1}} \int_0^\infty d\lambda\, \lambda \left[ I_{-\nu}(\eta\lambda) K_\nu(\eta'\lambda) + K_\nu(\eta\lambda) I_\nu(\eta'\lambda) \right] \sum_{\mathbf{n}_q} e^{i n_r \alpha_r} \\ &\times e^{i\mathbf{k}_{q-1}\cdot\Delta\mathbf{x}_{q-1}} \left(\lambda^2 + \mathbf{k}_{q-1}^2\right)^{\frac{p-1}{2}} f_{\frac{p-1}{2}}\left(\sqrt{\lambda^2 + \mathbf{k}_{q-1}^2} \sqrt{|\Delta\mathbf{x}_p|^2 + (\Delta x^r - n_r L_r)^2}\right), \end{aligned} \tag{44}$$

where $I_\nu(y)$ and $K_\nu(y)$ are the modified Bessel functions. Similar to the case of the Minkowski bulk, the contribution coming from the term $n_r = 0$ gives the Hadamard function for the geometry where the $r$th coordinate is decompactified (spatial topology $R^{p+1} \times T^{q-1}$). The effects of the compactification of that coordinate are included in the part with $n_r \neq 0$.

For a conformally coupled mass-less field, we have $\nu = 1/2$ and

$$I_{-\nu}(\eta\lambda) K_\nu(\eta'\lambda) + K_\nu(\eta\lambda) I_\nu(\eta'\lambda) = \frac{\cosh(\lambda\Delta\eta)}{\lambda\sqrt{\eta\eta'}}. \tag{45}$$

With this function, the integral over $z$ in (44) is evaluated by using the formula from [87], and we obtain

$$G(x,x') = \left(\frac{\eta\eta'}{a^2}\right)^{\frac{D-1}{2}} G_{\mathrm{M}}(x,x'), \tag{46}$$

where the Minkowskian Hadamard function $G_{\mathrm{M}}(x,x')$ is given by (21) with $m = 0$. For a conformally coupled mass-less field, this is the standard relation between two conformally related geometries.

### 4.2. Vacuum Current

For the components of the current density along non-compact dimensions $x^\mu$, $\mu = 1, 2, \ldots, p$, one has $\partial_\mu G(x,x') \propto g_{\mu\alpha}\Delta x^\alpha$ and the corresponding expectation values vanish. By using the properties of the modified Bessel functions, we can see that

$$\lim_{x'\to x} (\partial_0 - \partial_0') \left\{ (\eta\eta')^{\frac{D}{2}} \left[ I_{-\nu}(\eta\lambda) K_\nu(\eta'\lambda) + K_\nu(\eta\lambda) I_\nu(\eta'\lambda) \right] \right\} = 0, \tag{47}$$

and, hence, the charge density vanishes as well. In order to find the component of the current density along the $r$th compact dimension, we use the representation (44) for the Hadamard function in combination with (7), where $D_\mu = \partial_\mu$. In (44), the derivative of the term $n_r = 0$ with respect to $x^r$ is an odd function of $\Delta x^r$ and vanishes in the coincidence limit. As has been mentioned before, that term corresponds to the Hadamard function in the geometry with non-compactified $x^r$ and the corresponding current density vanishes by the symmetry. The part in (44), induced by the compactification of the direction $x^r$ (the terms with $n_r \neq 0$), is finite in the coincidence limit and that limit can be directly taken in the expression for the VEV. This gives the following expression for the contravariant component [22]:

$$\begin{aligned} \langle j^r \rangle &= \frac{8ea(\eta/a)^{D+2}}{(2\pi)^{\frac{p+3}{2}} V_q} L_r^2 \int_0^\infty d\lambda\, \lambda [I_{-\nu}(\eta\lambda) + I_\nu(\eta\lambda)] K_\nu(\eta\lambda) \\ &\times \sum_{n_r=1}^{\infty} n_r \sin(n_r \tilde{\alpha}_r) \sum_{\mathbf{n}_{q-1}} \left(\lambda^2 + \mathbf{k}_{q-1}^2\right)^{\frac{p+1}{2}} f_{\frac{p+1}{2}}\left(n_r L_r \sqrt{\lambda^2 + \mathbf{k}_{q-1}^2}\right). \end{aligned} \tag{48}$$

An alternative representation for the current density is obtained through Formula (35) with $s = p$. This gives

$$\langle j^r \rangle = \frac{4eL_r}{(2\pi)^{\frac{D}{2}+1} a^{D+1}} \int_0^\infty du\, u^{D+1} [I_{-\nu}(u) + I_\nu(u)] K_\nu(u) \sum_{\mathbf{n}_q} n_r \sin(\mathbf{n}_q \cdot \tilde{\boldsymbol{\alpha}}_q) f_{\frac{D}{2}}(ug(\mathbf{L}_q, \mathbf{n}_q)/\eta). \tag{49}$$

The integral in the right-hand side is evaluated by using the formula

$$\int_0^\infty dz\, z^{\frac{D}{2}+1} [I_\nu(z) + I_{-\nu}(z)] K_\nu(z) K_{\frac{D}{2}}(bz) = \frac{\sqrt{2\pi}}{4} b^{\frac{D}{2}} p_{\nu-\frac{1}{2}}^{-\frac{D+1}{2}} \left( \frac{b^2}{2} - 1 \right), \tag{50}$$

where we use the notation

$$p_\alpha^{-\mu}(u) = \Gamma(\mu - \alpha)\Gamma(\mu + \alpha + 1) \frac{P_\alpha^{-\mu}(u)}{(u^2 - 1)^{\frac{\mu}{2}}}, \tag{51}$$

with $P_\nu^\mu(u)$ being the associated Legendre function of the first kind. The expression of the function $p_\alpha^{-\mu}(u)$ in terms of the hypergeometric function is given in Appendix A. The result (50) is obtained from the integral involving the product $I_\nu(z) K_\nu(z) K_{\frac{D}{2}}(bz)$ and given in [87]. That integral is expressed in terms of the sum of two hypergeometric functions. The contribution of the second function is canceled in evaluating the integral (50). Then, we express the hypergeometric function in terms of the associated Legendre functions. By taking into account (50) in (49), the current density is expressed as

$$\langle j^r \rangle = \frac{eL_r}{(2\pi)^{\frac{D+1}{2}} a^{D+1}} \sum_{\mathbf{n}_q} n_r \sin(\mathbf{n}_q \cdot \tilde{\boldsymbol{\alpha}}_q) p_{\nu-\frac{1}{2}}^{-\frac{D+1}{2}} \left( \frac{g^2(\mathbf{L}_q, \mathbf{n}_q)}{2\eta^2} - 1 \right). \tag{52}$$

In both Formulas (49) and (52), we can make the replacement (34). Note that one has the property $p_{\nu-\frac{1}{2}}^{-\frac{D+1}{2}}(u) = p_{-\nu-\frac{1}{2}}^{-\frac{D+1}{2}}(u)$ and the expression on the right-hand side is real for both the real and the purely imaginary values of $\nu$.

## 5. AdS Spacetime with Compact Dimensions

Now we turn to the LAdS spacetime with a part of the spatial dimensions compactified to a torus. This obeys the $(D+1)$-dimensional Einstein equations with the negative cosmological constant $\Lambda$. The usual AdS spacetime is maximally symmetric and appears as the ground state in supergravity and in string theories. That was the reason for the early interest in AdS physics. The interest in those investigations was further increased as a result of two exciting developments in modern theoretical physics. The first one, dubbed as AdS/CFT correspondence (see, for example, [88–91]), establishes a duality between supergravity and string theory on the AdS bulk and conformal field theory (CFT) on its boundary. This duality is a unique way to investigate strong coupling effect in one theory by mapping it onto the dual theory. A number of examples can be found in the literature, including those with applications in condensed matter physics. The second development, with the AdS spacetime as a background geometry, corresponds to braneworld models of the Randall–Sundrum type [92], with large extra dimensions. In the corresponding setup, the standard model fields are localized in a four-dimensional hypersurface (brane) in the context of a higher-dimensional AdS spacetime. The braneworld models provide a geometrical solution to the hierarchy problem between the electroweak and Planck energy scales and naturally arise in the string/M theory context. They present a novel setting in considerations of various phenomenological and cosmological issues, in particular, the generation of a cosmological constant localized on the brane.

By the analogy of the dS bulk, it is convenient to visualize the AdS spacetime as a hyperboloid

$$\left(Z^0\right)^2 - \sum_{i=1}^{D} \left(Z^i\right)^2 + \left(Z^{D+1}\right)^2 = -a^2, \tag{53}$$

where the line element of the embedding $(D+2)$-dimensional flat spacetime is given by $ds^2_{D+2} = (dZ^0)^2 - \sum_{i=1}^{D}(dZ^i)^2 + (dZ^{D+1})^2$. The Poincaré coordinates $(t, x^1 = z, x^2, \ldots, x^D)$ are introduced by the relations

$$\begin{aligned} Z^i &= \frac{1}{2z}\left[a^2 + (-1)^i\left(\sum_{l=1}^{D}(x^l)^2 - t^2\right)\right],\ i = 0, 1, \\ Z^l &= \frac{a}{z}x^l,\ Z^{D+1} = \frac{a}{z}t,\ l = 2, \ldots, D. \end{aligned} \tag{54}$$

In those coordinates, the metric tensor of the AdS spacetime is expressed as

$$g_{\mu\nu} = \frac{a^2}{z^2}\eta_{\mu\nu}, \tag{55}$$

with $0 \le z < \infty$. The hypersurfaces $z = 0$ and $z = \infty$ present the AdS boundary and the horizon, respectively. The proper distance along the direction $x^1$ is measured by the coordinate $y = a\ln(z/a)$, $-\infty < y < +\infty$; in terms of this, the line element is written as

$$ds^2 = \exp\left(-\frac{2y}{a}\right)\left[dt^2 - \sum_{l=2}^{D}(dx^l)^2\right] - dy^2. \tag{56}$$

Here, we consider the LAdS geometry with the coordinates $(x^{p+1}, x^{p+2}, \ldots, x^D)$ compactified to a torus, as described in Section 2. It can be embedded as a hyperboloid (53) in the spacetime with coordinates $(Z^0, Z^1, \ldots, Z^{D+1})$, where the coordinate $Z^l$, $l = p+1, \ldots, D$ is compactified to a circle with the length $L_{(\mathrm{p})l} = aL_l/z = e^{-y/a}L_l$. The latter is the proper length for the compact dimension in LAdS. It is exponentially small near the horizon.

The scalar mode functions in the coordinates corresponding to the metric tensor (55) and obeying the periodicity conditions (13) are written in the factorized form $\varphi_\sigma^{(\pm)}(x) = e^{\mp i\omega t + i\mathbf{k}_{p-1}\mathbf{x}_{p-1} + \mathbf{k}_q\mathbf{x}_q}f(z)$, with $\mathbf{x}_{p-1} = (x^2, \ldots, x^p)$, $\mathbf{k}_{p-1} = (k_2, \ldots, k_p)$. The equation for the function $f(z)$ is obtained from the field equation. The corresponding solution is presented as $z^{D/2}[c_1 J_{\nu_+}(\lambda z) + c_2 Y_{\nu_+}(\lambda z)]$, where $J_\nu(\lambda z)$ and $Y_\nu(\lambda z)$ are the Bessel and Neumann functions, $\lambda^2 = \omega^2 - \mathbf{k}_{p-1}^2 - \mathbf{k}_q^2$, and

$$\nu_+ = \left[\frac{D^2}{4} - D(D+1)\xi + a^2m^2\right]^{1/2}. \tag{57}$$

For the stability of the Poincaré vacuum, the parameter $\nu_+$ should be real [93–95]. For $\nu_+ \ge 1$ from the normalizability condition, it follows that $c_2 = 0$ in the linear combination of the cylinder functions. For $0 \le \nu_+ < 1$, the modes with $c_2 \ne 0$ are normalizable. In this case, one of the coefficients in the linear combination is determined from the normalization condition and the second one is fixed by the boundary condition on the AdS boundary. This general class of allowed boundary conditions was discussed in [96,97]. Here, we will consider the special case of the Dirichlet boundary condition, for which $c_2 = 0$ and $f(z) = c_1 z^{D/2}J_{\nu_+}(\lambda z)$. The normalized mode functions are expressed as

$$\varphi_\sigma^{(\pm)}(x) = \left(\frac{\pi^{-p}a^{1-D}\lambda}{2^{p+1}\omega V_q}\right)^{\frac{1}{2}} z^{\frac{D}{2}} e^{i\mathbf{k}_{p-1}\mathbf{x}_{p-1} + i\mathbf{k}_q\mathbf{x}_q \mp i\omega t} J_{\nu_+}(\lambda z). \tag{58}$$

The modes are specified by the set $\sigma = (\lambda, \mathbf{k}_{p-1}, \mathbf{k}_q)$ with $0 \le \lambda < \infty$, and the energy is given by $\omega = \sqrt{\lambda^2 + \mathbf{k}_{p-1}^2 + \mathbf{k}_q^2}$.

With the mode functions (58), the Hadamard function takes the form

$$G(x,x') = \frac{a^{1-D}(zz')^{\frac{D}{2}}}{(2\pi)^{p-1}V_q}\sum_{\mathbf{n}_q}\int d\mathbf{k}_{p-1}\, e^{i\mathbf{k}_{p-1}\cdot\Delta\mathbf{x}_{p-1}+i\mathbf{k}_q\cdot\Delta\mathbf{x}_q}\int_0^\infty d\lambda\,\frac{\lambda}{\omega}J_{\nu_+}(\lambda z)J_{\nu_+}(\lambda z')\cos(\omega\Delta t). \tag{59}$$

Similar to the cases of the locally Minkowski and dS geometries, we apply the series over $n_r$, the summation Formula (20), to determine the representation

$$\begin{aligned} G(x,x') \;=\; & \frac{2(zz')^{\frac{D}{2}}L_r}{(2\pi)^{\frac{p+1}{2}}V_q a^{D-1}}\sum_{\mathbf{n}_q} e^{i\mathbf{k}_{q-1}\cdot\Delta\mathbf{x}_{q-1}+in_r\tilde{\alpha}_r}\int_0^\infty d\lambda\,\lambda J_{\nu_+}(\lambda z)J_{\nu_+}(\lambda z')\left(\lambda^2+\mathbf{k}_{q-1}^2\right)^{\frac{p-1}{2}} \\ & \times f_{\frac{p-1}{2}}\left(\sqrt{\lambda^2+\mathbf{k}_{q-1}^2}\sqrt{|\Delta\mathbf{x}_{p-1}|^2+(\Delta x^r-n_rL_r)^2-(\Delta t)^2}\right). \end{aligned} \tag{60}$$

The term with $n_r = 0$ in this representation corresponds to the Hadamard function in the geometry where the $r$th dimension is decompactified.

Another representation for the function (59) is obtained in [23] by using an integral representation for the ratio $\cos(\omega\Delta t)/\omega$. The integral over $\lambda$ is expressed in terms of the modified Bessel function. Integrating over the components of the momentum along non-compact dimensions and applying the Poisson resummation formula to the series, the Hadamard function is expressed as

$$G(x,x') = \frac{a^{1-D}}{(2\pi)^{D/2}}\sum_{\mathbf{n}_q} e^{i\tilde{\text{ff}}\cdot\mathbf{n}_q}\int_0^\infty dx\, x^{D/2-1}I_\nu(x)e^{-v_{\mathbf{n}_q}x}, \tag{61}$$

where

$$v_{\mathbf{n}_q} = 1+\frac{1}{2zz'}\left[(\Delta z)^2+(\Delta\mathbf{x}_{p-1})^2+\sum_{i=p+1}^{D}\left(\Delta x^i-L_in_i\right)^2-(\Delta t)^2\right], \tag{62}$$

and $\Delta z = z - z'$. By using the result from [87] for the integral in (61), the following representation is obtained:

$$G(x,x') = \frac{2a^{1-D}}{(2\pi)^{\frac{D+1}{2}}}\sum_{\mathbf{n}_q} e^{i\tilde{\text{ff}}\cdot\mathbf{n}_q} q_{\nu_+-\frac{1}{2}}^{\frac{D-1}{2}}(v_{\mathbf{n}_q}), \tag{63}$$

where the function $q_\alpha^\mu(x)$ is expressed in terms of the associated Legendre function of the second kind, $Q_\alpha^\mu(x)$ (for the expression in terms of the hypergeometric function, see Appendix A):

$$q_{\nu-\frac{1}{2}}^{\mu}(x) = \frac{e^{-i\pi\mu}Q_{\nu-\frac{1}{2}}^{\mu}(x)}{(x^2-1)^{\frac{\mu}{2}}}. \tag{64}$$

The contribution in (63), corresponding to the term $\mathbf{n}_q = 0$, presents the Hadamard function in AdS spacetime with Poincaré coordinates $-\infty < x^\mu < +\infty$ for $\mu = 2,3,\ldots,D$. The divergences in the coincidence limit are contained in that part. The topological contribution with $\mathbf{n}_q \neq 0$ is finite in that limit and can be directly used in evaluating the current density.

As before, the charge density and the components of the current density along non-compact dimensions vanish: $\langle j^\mu\rangle = 0$ for $\mu = 0,1,\ldots,p$. Combining Formulas (7) and (60), for the component along the $r$th dimension, we find

$$\langle j^r\rangle = \frac{4ez^{D+2}L_r^2}{(2\pi)^{\frac{p+1}{2}}a^{D+1}V_q}\sum_{n_r=1}^{\infty} n_r\sin(n_r\tilde{\alpha}_r)\sum_{\mathbf{n}_{q-1}}\int_0^\infty d\lambda\,\lambda J_{\nu_+}^2(\lambda z)\left(\lambda^2+\mathbf{k}_{q-1}^2\right)^{\frac{p+1}{2}} f_{\frac{p+1}{2}}\left(n_rL_r\sqrt{\lambda^2+\mathbf{k}_{q-1}^2}\right). \tag{65}$$

By applying Formula (35) with $s = p$ to the series over $\mathbf{n}_{q-1}$, one obtains

$$\langle j^r\rangle = \frac{4ez^{D+2}L_r}{(2\pi)^{\frac{D}{2}}a^{D+1}}\sum_{n_r=1}^{\infty} n_r \sin(n_r\tilde{\alpha}_r)\sum_{\mathbf{n}_{q-1}}\cos(\mathbf{n}_{q-1}\cdot\tilde{\boldsymbol{\alpha}}_{q-1})\int_0^{\infty} d\lambda\,\lambda^{D+1}J^2_{\nu_+}(\lambda z)f_{\frac{D}{2}}(\lambda g(\mathbf{L}_q,\mathbf{n}_q)). \tag{66}$$

The integral in (66) is expressed in terms of the function (64) [98] (note that there is a misprint in the similar integral given in [87]) and the current density is presented in the form [23]

$$\langle j^r\rangle = \frac{4eL_r}{(2\pi)^{\frac{D+1}{2}}a^{D+1}}\sum_{n_r=1}^{\infty} n_r \sin(\tilde{\alpha}_r n_r)\sum_{\mathbf{n}_{q-1}}\cos(\mathbf{n}_{q-1}\cdot\tilde{\boldsymbol{\alpha}}_{q-1})q^{\frac{D+1}{2}}_{\nu_+-\frac{1}{2}}\left(1+\frac{g^2(\mathbf{L}_q,\mathbf{n}_q)}{2z^2}\right). \tag{67}$$

This representation could be directly obtained using the Hadamard function in the form (63) and the relation $\partial_x q^{\mu}_{\alpha}(x) = -q^{\mu+1}_{\alpha}(x)$ for the function (64).

## 6. Features of the Current Density

### *6.1. General Features*

The physical component of the charge density is given by $\left\langle j^r_{(\mathrm{p})}\right\rangle = \sqrt{|g_{rr}|}\langle j^r\rangle$. It determines the charge flux through the spatial hypersurface $x^r = \mathrm{const}$, expressed as $n_r\langle j^r\rangle$, with $n_r = \sqrt{|g_{rr}|}$ being the corresponding normal. The expressions obtained above for the $r$th component of the current density can be combined as

$$\left\langle j^r_{(\mathrm{p})}\right\rangle = \frac{2eL_{(\mathrm{p})r}}{(2\pi)^{\frac{D+1}{2}}a^{D+1}}\sum_{\mathbf{n}_q} n_r \sin(\mathbf{n}_q\cdot\tilde{\boldsymbol{\alpha}}_q)F_D(am, g(\mathbf{L}_{(\mathrm{p})q}/a,\mathbf{n}_q)), \tag{68}$$

where we have defined the function

$$\begin{aligned} F_D(am,x) &= (am)^{D+1}f_{\frac{D+1}{2}}(amx),\ \text{for LM},\\ F_D(am,x) &= \sqrt{\frac{2}{\pi}}\int_0^{\infty} du\,u^{D+1}Z(u)f_{\frac{D}{2}}(ux),\ \text{for LdS, LAdS,} \end{aligned} \tag{69}$$

with

$$\begin{aligned} Z(u) &= [I_{-\nu}(u)+I_{\nu}(u)]K_{\nu}(u),\ \text{for LdS},\\ Z(u) &= \pi J^2_{\nu_+}(u),\ \text{for LAdS}. \end{aligned} \tag{70}$$

Alternative expressions for locally dS and AdS geometries are obtained from (52) and (67):

$$\begin{aligned} F_D(am,x) &= \frac{1}{2}P^{-\frac{D+1}{2}}_{\nu-\frac{1}{2}}\left(x^2/2-1\right),\ \text{for LdS},\\ F_D(am,x) &= q^{\frac{D+1}{2}}_{\nu_+-\frac{1}{2}}\left(x^2/2+1\right),\ \text{for LAdS}. \end{aligned} \tag{71}$$

For even values of the spatial dimension $D$, the functions (71) are expressed in terms of elementary functions. The corresponding representations are given by Formulas (A4) and (A5). In an odd number of spatial dimensions, the expressions for the functions (71), in terms of the Legendre functions $P_{\nu-\frac{1}{2}}(u)$ and $Q_{\nu_+-\frac{1}{2}}(u)$, are given by (A6).

In asymptotic analysis for some limiting cases, it is more convenient to use the representations (22), (48) and (65). For LdS and LAdS geometries, the corresponding formulas can be combined by using (70):

$$\left\langle j_{(\mathrm{p})}^{r}\right\rangle = \frac{8ea^{-p-2}L_{(\mathrm{p})r}^{2}}{(2\pi)^{\frac{p+3}{2}}V_{q}^{(\mathrm{p})}}\sum_{n_r=1}^{\infty}n_r\sin(n_r\tilde{\alpha}_r)\sum_{\mathbf{n}_{q-1}}\int_0^{\infty}du\,uZ(u) \times\left(u^2+a^2\mathbf{k}_{q-1}^{(\mathrm{p})2}\right)^{\frac{p+1}{2}}f_{\frac{p+1}{2}}\left(n_rL_{(\mathrm{p})r}/a\sqrt{u^2+a^2\mathbf{k}_{q-1}^{(\mathrm{p})2}}\right). \quad (72)$$

with the notation

$$\mathbf{k}_{q-1}^{(\mathrm{p})2} = \sum_{i=p+1,\neq r}^{D}\left(\frac{2\pi n_i+\tilde{\alpha}_i}{L_{(\mathrm{p})i}}\right)^2. \quad (73)$$

Note that the vector $\mathbf{k}_{q-1}^{(\mathrm{p})}$ is the physical momentum in the compact sub-space with the set of coordinates $(x^{p+1},\ldots,x^{r-1},x^{r+1},\ldots,x^{D})$.

First of all, we see that the current density along the $r$th dimension is an even periodic function of the parameters $\tilde{\alpha}_i$, $i\neq r$, with the period $2\pi$ and an odd periodic function of $\tilde{\alpha}_r$ with the same period. This corresponds to the periodicity with respect to the magnetic flux, with the period equal to the flux quantum. From Formula (68), it follows that the physical component $n_r\langle j^r\rangle$ depends on the lengths of compact dimensions and on the coordinates through the ratios $L_{(\mathrm{p})i}/a$, $i=p+1,\ldots,D$. They present the proper lengths of compact dimensions measured in units of the curvature radius. This feature is related to the maximal symmetry of the dS and AdS spacetimes.

The numerical examples below will be given for models with a single compact dimension $x^D$ having the length $L=L_D$. In Figure 1, we present the dependence of the respective current density, multiplied by $L_{(\mathrm{p})}^{D}/e$, as a function of the parameter $\tilde{\alpha}_D/(2\pi)$ and of the proper length of the compact dimension $L_{(\mathrm{p})}=L_{(\mathrm{p})D}$ in the LM spacetime with $D=4$. In the numerical evaluation, we have taken $ma=0.5$. In the LM bulk, the current density does not depend on the curvature coupling parameter and $L_{(\mathrm{p})}=L$. As follows from (24), for a mass-less field, the dimensionless combination $L_{(\mathrm{p})}^{D}\left\langle j_{(\mathrm{p})}^{D}\right\rangle/e$ does not depend on $L_{(\mathrm{p})}$.

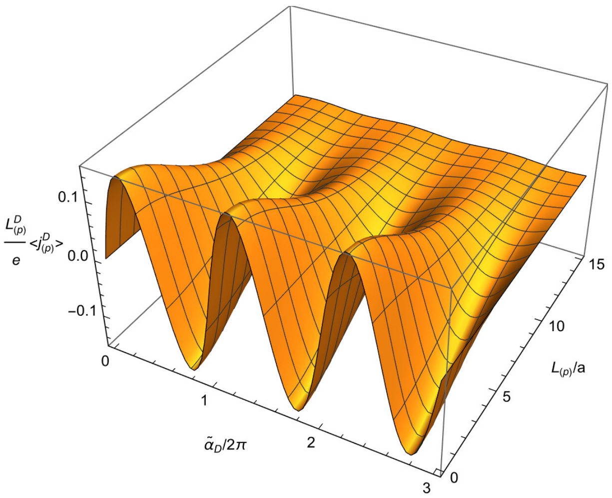


**Figure 1.** The current density in the $D=4$ LM spacetime versus the parameter $\tilde{\alpha}_D/(2\pi)$ and the proper length of the compact dimension (in units of $a$). The graph is plotted for $ma=0.5$.

The current densities for the $D=4$ LdS and LAdS background geometries and for $ma=0.5$ are plotted in Figures 2 and 3. The left and right panels on both figures correspond to conformally and minimally coupled fields.

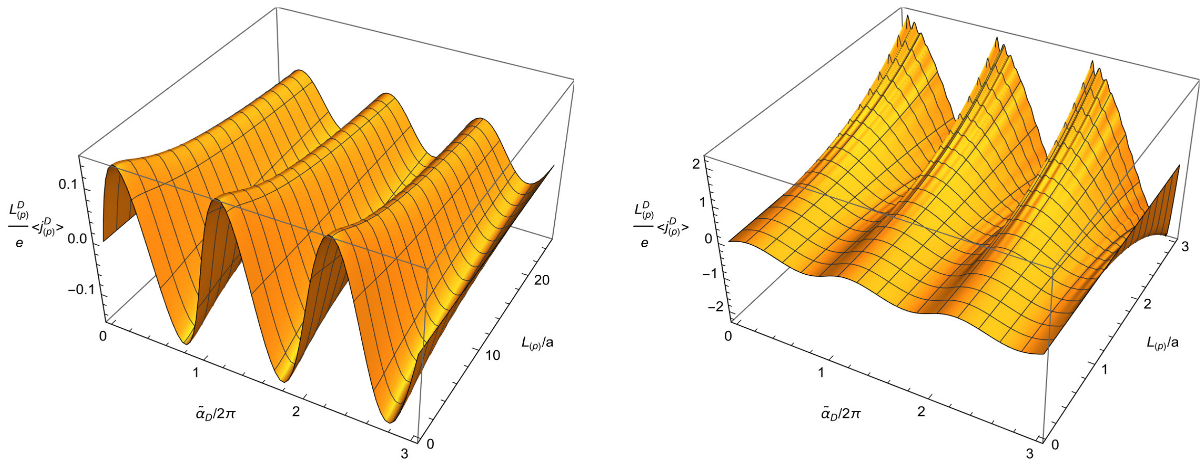


**Figure 2.** The current density in the $D = 4$ LdS spacetime, multiplied by $L_{(\mathrm{p})}^{D}/e$, versus the parameter $\tilde{\alpha}_D/(2\pi)$ and the proper length of the compact dimension for $ma = 0.5$. The left and right panels correspond to conformally and minimally coupled fields, respectively.

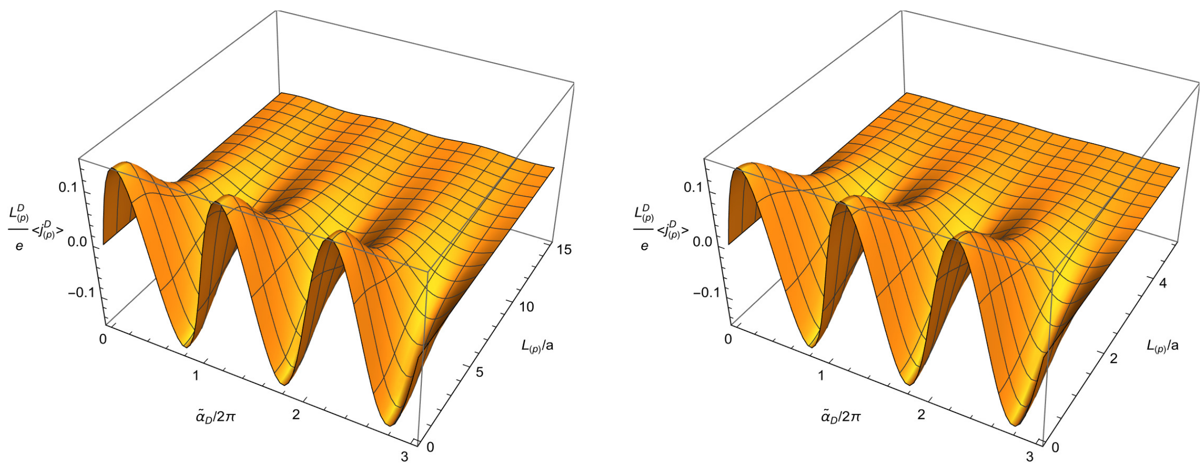


**Figure 3.** The same as in Figure 2 for the LAdS bulk.

### 6.2. Conformal Coupling and Minkowskian Limit

Let us consider special cases of general formulas. For a conformally coupled mass-less field, one has $\xi = \xi_D$ and $\nu = \nu_+ = 1/2$. The current density for the Minkowskian case does not depend on the curvature coupling parameter; from (33), we obtain

$$\langle j^r \rangle_{\mathrm{LM}} = eL_r \frac{\Gamma\left(\frac{D+1}{2}\right)}{\pi^{\frac{D+1}{2}}} \sum_{\mathbf{n}_q} \frac{n_r \sin\left(\mathbf{n}_q \cdot \tilde{\boldsymbol{\alpha}}_q\right)}{g^{D+1}(\mathbf{L}_q, \mathbf{n}_q)}. \tag{74}$$

The corresponding functions $F_D(am, x)$ for dS and AdS geometries are obtained from (69) by taking into account that $[I_{-\nu}(u) + I_\nu(u)]K_\nu(u) = 1/u$ for $\nu = 1/2$ and $J_{\nu_+}(u) = \sqrt{2/\pi u}\sin u$ for $\nu_+ = 1/2$. The integrals are evaluated using the formulas from [87] and we obtain

$$\begin{aligned} \langle j^r \rangle_{\mathrm{LdS}} &= \left(\frac{\eta}{a}\right)^{D+1} \langle j^r \rangle_{\mathrm{LM}}, \\ \langle j^r \rangle_{\mathrm{LAdS}} &= \left(\frac{z}{a}\right)^{D+1} \langle j^r \rangle_{\mathrm{LM}}^{(1)}, \end{aligned} \tag{75}$$

where

$$\langle j^r \rangle^{(1)}_{\rm LM} = eL_r \frac{\Gamma\left(\frac{D+1}{2}\right)}{\pi^{\frac{D+1}{2}}} \sum_{\mathbf{n}_q} n_r \sin\left(\mathbf{n}_q \cdot \tilde{\boldsymbol{\alpha}}_q\right) \left[ \frac{1}{g^{D+1}(\mathbf{L}_q, \mathbf{n}_q)} - \frac{1}{\left(4z^2 + g^2(\mathbf{L}_q, \mathbf{n}_q)\right)^{\frac{D+1}{2}}} \right]. \quad (76)$$

The result (75) for the dS bulk was expected from the conformal relation between the problems in the Minkowski and dS geometries with the same range of the spatial coordinates and between the Bunch–Davies and Minkowski vacua. For the AdS bulk, the contribution of the first term in the square brackets of (76) will give the Minkowskian current density multiplied by the conformal factor $(z/a)^{D+1}$. The presence of the part coming from the second term in the square brackets is related to the boundary condition on the AdS boundary at $z = 0$. Because of that condition, the problem on the AdS bulk for a conformally coupled mass-less field is conformally related to the corresponding problem in the Minkowski bulk with an additional boundary at $z = 0$, with the Dirichlet boundary condition for the field. The VEV (76) is the current density for a conformally coupled mass-less field in the region $0 < z < \infty$ of the locally Minkowski bulk with Dirichlet boundary at $z = 0$.

In Figure 4, for a mass-less field, we have plotted the dependence of the ratios $\langle j^D \rangle_{\rm LAdS} / \langle j^D \rangle_{\rm LM}$ and $\langle j^D \rangle_{\rm LdS} / \langle j^D \rangle_{\rm LM}$ on the proper length $L_{(\rm p)} = L_{(\rm p)D}$ of a single compact dimension (in units of the curvature radius $a$). It is assumed that the compact dimension has the same proper length in LAdS, LdS, and LM spacetimes. The left and right panels correspond to conformally and minimally coupled fields, respectively, and the numbers near the curves present the values of the respective spatial dimension. For a conformally coupled field, $\langle j^D \rangle_{\rm LdS} / \langle j^D \rangle_{\rm LM} = 1$; only the case of the LAdS bulk is depicted on the left panel. The full and dashed curves on the right panel correspond to the LAdS and LdS geometries, respectively. As seen from the graphs, for mass-less fields, the decay of the current density—as a function of the proper length of the compact dimension—is stronger in the LAdS spacetime (compared to the case of the LM bulk). For a minimally coupled field in the LdS geometry, the fall-off of the current density is stronger in the LM spacetime. For small values of the proper length, compared to the curvature radius, the effect of the gravitational field is weak and the ratio $\langle j^D \rangle / \langle j^D \rangle_{\rm LM}$ tends to 1. All these features will be confirmed below by asymptotic analysis.

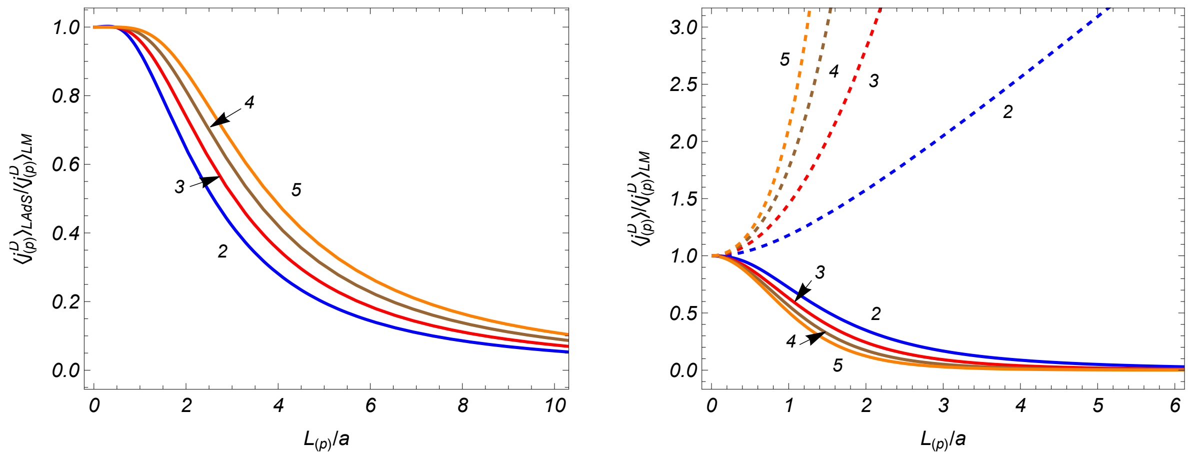


**Figure 4.** The left panel presents the ratio of the current densities for a conformally coupled mass-less scalar field in LAdS and LM spacetimes, with a single compact dimension of the proper length $L_{(\rm p)} = L_{(\rm p)D}$, versus the ratio $L_{(\rm p)}/a$. On the right panel, the ratio $\langle j^D \rangle / \langle j^D \rangle_{\rm LM}$ is plotted for a minimally coupled mass-less scalar field in LAdS (full curves, $\langle j^D \rangle = \langle j^D \rangle_{\rm LAdS}$) and LdS (dashed curves, $\langle j^D \rangle = \langle j^D \rangle_{\rm LdS}$). The numbers near the curves present the corresponding spatial dimension. The different behaviors for the LAdS and LdS geometries in the regions of large compact dimensions will be clarified below using asymptotic analysis.

Now, let us check the Minkowskian limit for dS and AdS geometries. As seen from (40) and (56), it is obtained taking $a \to \infty$ for fixed spacetime coordinates $(t, x^1, \ldots, x^D)$ and $(t, y, x^2, \ldots, x^D)$ for the dS and AdS cases, respectively. For a large curvature radius, one has $\nu \approx iam$, $\eta \approx a - t$ in LdS bulk and $\nu_+ \approx am$, $z \approx a + y$ for LAdS. In the case of LAdS, we need the asymptotic expression of the function $q^{(D+1)/2}_{\nu_+-1/2}(u^2/2+1)$ for $\nu_+ \gg 1$ and $u \ll 1$. That expression is obtained using the uniform asymptotic expression of the associated Legendre function of the second kind for large degree and fixed order, given in [99]. With that asymptotic, it can be checked that, in the limit under consideration

$$q^{\frac{D+1}{2}}_{\nu_+-1/2}\left(1 + \frac{g^2(\mathbf{L}_{(\mathrm{p})q}, \mathbf{n}_q)}{2a^2}\right) \approx (am)^{D+1} f_{\frac{D+1}{2}}(mg(\mathbf{L}_q, \mathbf{n}_q)), \tag{77}$$

confirming the transition to the Minkowskian result. In the case of LdS, it is convenient to use the representation (69) for the function $F_D(am, x)$. In the limit at hand, $\nu \approx iam$, $am \gg 1$. The corresponding uniform asymptotic expansions for the functions $I_{\pm\nu}(u)$ and $K_\nu(u)$ can be found, for example, in [100,101]. From those expansions, it can be seen that the dominant contribution to the integral in the expression for $F_D(am, x)$ comes from the region $u > am$, where

$$[I_\nu(u) + I_{-\nu}(u)]K_\nu(u) \sim \frac{1}{\sqrt{u^2 - a^2m^2}}. \tag{78}$$

with $\nu \approx iam$. The respective integral is evaluated by using the formula

$$\int_0^\infty du \left(u^2 + b^2\right)^\mu f_\mu(c\sqrt{u^2 + b^2}) = \sqrt{\frac{\pi}{2}} b^{2\mu+1} f_{\mu+\frac{1}{2}}(cb), \tag{79}$$

and we see that, for the leading order

$$F_D(am, x) \approx (ma)^{D+1} f_{\frac{D+1}{2}}(max), \tag{80}$$

which coincides with the Minkowskian result.

### *6.3. Large and Small Proper Lengths of Compact Dimensions*

For small values of the proper length of the $r$th compact dimension, $L_{(\mathrm{p})r} \ll a, 1/m$, we first consider the contribution in (68) of the terms for which at least one of $n_i$, $i \neq r$ is different from zero. For that part, the dominant contribution to the series over $n_r$ comes from the terms with large values $|n_r|$; we replace the corresponding summation with the integration. The corresponding integral involving the product of the sin and Macdonald functions is evaluated by using the formula from [98] and is expressed in terms of the Macdonald function with much disagreement. By using the corresponding asymptotic, we see that the contribution of the term for which at least one of $n_i$, $i \neq r$ is not zero, is suppressed by the factor $\exp[-g(\mathbf{L}_{(\mathrm{p})q-1}/a, \mathbf{n}_{q-1})\tilde{\alpha}_r a/L_{(\mathrm{p})r}]$, where

$$g^2(\mathbf{L}_{(\mathrm{p})q-1}/a, \mathbf{n}_{q-1}) = \sum_{i=p+1,\neq r}^{D} n_i^2 \frac{L_i^2}{a^2}. \tag{81}$$

For the contribution of the terms with $n_i = 0$, $i \neq r$, in (68), the argument $x$ of the function $F_D(am, x)$ is small. By using the corresponding asymptotic for the Macdonald function, we see that, in the case of LM bulk

$$F_D(am, x) \approx \frac{2^{\frac{D-1}{2}}}{x^{D+1}} \Gamma\left(\frac{D+1}{2}\right), \; x \ll 1. \tag{82}$$

In the cases of the LdS and LAdS geometries, we note that the main contribution to the integrals in (69) comes from the region with large values of $u$. By using the respective approximations for the functions $[I_{-\nu}(u)+I_{\nu}(u)]K_{\nu}(u)$ and $J^2_{\nu_+}(u)$ and evaluating the integrals, we can see that the corresponding asymptotics are given by the same expression (82). Hence, in the limit $L_{(\mathrm{p})r} \ll a, 1/m$, the dominant contribution to the current density comes from the modes with $n_i = 0$, $i \neq r$, and to the leading order

$$\left\langle j^r_{(\mathrm{p})} \right\rangle \approx \frac{2e\Gamma\left(\frac{D+1}{2}\right)}{\pi^{\frac{D+1}{2}} L^D_{(\mathrm{p})r}} \sum_{n_r=1}^{\infty} \frac{\sin(n_r\tilde{\alpha}_r)}{n_r^D}. \tag{83}$$

The expression in the right-hand side presents the current density for a mass-less scalar field in the LM spacetime with spatial topology $R^{D-1}\times S^1$, with a single compact dimension $x^r$ with length $L_r = L_{(\mathrm{p})r}$. For small values of $L_{(\mathrm{p})r}$, the dominant contribution to the VEVs comes from the vacuum fluctuations with small values of the wavelength (compared to the curvature radius) and the effects of gravity are weak.

It is expected that the effects of gravity on the vacuum currents will be essential for proper lengths of compact dimensions of the order of or larger than the curvature radius. We start a consideration of the large values of the lengths with the LM case, assuming that $L_r$ is much larger than the other length scales of the model. From Formula (22), it follows that the dominant contribution comes from the modes with $n_i = 0$, $i \neq r$, for which $\omega_{\mathbf{n}_{q-1}} = \omega_{0r} = \sqrt{k^{(0)2}_{\mathbf{n}_{q-1}} + m^2}$ with

$$k^{(0)2}_{\mathbf{n}_{q-1}} = \textstyle\sum_{l=p+1,\neq r}^{D} \tilde{\alpha}_l^2/L_l^2. \tag{84}$$

The behavior of the current density is essentially different depending whether $\omega_{0r}$ is zero or not. In the first case, the leading term in the current density is given as

$$\langle j^r \rangle_{\mathrm{LM}} \approx \frac{2e\Gamma(\frac{p}{2}+1)}{\pi^{\frac{p}{2}+1} L_r^p V_q} \sum_{n_r=1}^{\infty} \frac{\sin(n_r\tilde{\alpha}_r)}{n_r^{p+1}}. \tag{85}$$

Through a comparison with (83), we see that the right-hand side of (85), multiplied by $V_{q-1} = V_q/L_r$, presents the current density for a mass-less scalar field in $(p+2)$-dimensional LM spacetime with a spatial topology of $R^p \times S^1$, with a single compact dimension of $x^r$. For $\omega_{0r} \neq 0$, the dominant contribution to the current density is induced by the mode with $n_r = 1$ and, to the leading order,

$$\langle j^r \rangle_{\mathrm{LM}} \approx \frac{2e\sin(\tilde{\alpha}_r)\omega_{0r}^{\frac{p+1}{2}}}{(2\pi)^{\frac{p+1}{2}} L_r^{\frac{p-1}{2}} V_q} e^{-L_r\omega_{0r}}. \tag{86}$$

In particular, for the model with a single compact dimension $x^D$ one has $p = D-1$ and the asymptotic (86) takes the form

$$\left\langle j^D \right\rangle_{\mathrm{LM}} \approx \frac{2e\sin(\tilde{\alpha}_D)m^{\frac{D}{2}}}{(2\pi L_D)^{\frac{D}{2}}} e^{-mL_D}, \tag{87}$$

where $mL_D \gg 1$.

For LdS and LAdS geometries and for large values of the proper length $L_{(\mathrm{p})r}$ it is more convenient to use the representations (48) and (65). The dominant contribution comes from the term in the summation with $\mathbf{n}_{q-1} = 0$ ($n_l = 0$ for $l \neq r$) and from the integration region near the lower limit. Two cases should be considered separately. The first one corresponds to the phases $\tilde{\alpha}_i = 0$, $i \neq r$. With these values and for LAdS and LdS bulks in the case of $\nu > 0$, the leading order term is expressed as

$$\langle j^r_{(\mathrm{p})}\rangle \approx \frac{4ea^{1+2\mu}B_D(am)}{\pi^{\frac{p+1}{2}}V_q^{(\mathrm{p})}L_{(\mathrm{p})r}^{p+1+2\mu}}\Gamma\left(\frac{p+3}{2}+\mu\right)\sum_{n_r=1}^{\infty}\frac{\sin(n_r\tilde{\alpha}_r)}{n_r^{p+2+2\mu}}, \tag{88}$$

where

$$\mu = \begin{cases} -\nu, & \text{for LdS} \\ \nu_+, & \text{for LAdS} \end{cases}, \tag{89}$$

and

$$B_D(am) = \begin{cases} \Gamma(\nu)/(2\pi), & \text{for LdS} \\ 1/\Gamma(\nu_+ + 1), & \text{for LAdS} \end{cases}. \tag{90}$$

For LdS geometry and for imaginary values of $\nu$, $\nu = i|\nu|$, by similar calculations, the leading term is presented as

$$\left\langle j^r_{(\mathrm{p})}\right\rangle \approx \frac{4eC(ma)\eta^{D+1}}{\pi^{\frac{p+3}{2}}V_q a^D L_r^{p+1}}\sum_{n_r=1}^{\infty}\frac{\sin(n_r\tilde{\alpha}_r)}{n_r^{p+2}}\cos[2|\nu|\ln(n_rL_r/\eta)+\phi_0], \tag{91}$$

where the coefficient $C(ma) > 0$ and the phase $\phi_0$ are defined by the following relation

$$\Gamma(i|\nu|)\Gamma\left(\frac{p+3}{2}-i|\nu|\right) = C(ma)e^{i\phi_0}. \tag{92}$$

In this case, the current density exhibits an oscillatory behavior with the amplitude, decaying as $1/L_{(\mathrm{p})r}^{p+1}$. Comparing (88) and (91) with (86), we see that the gravitational field essentially modifies the asymptotic behavior of the current density for large values of the proper length $L_{(\mathrm{p})r}$: one has a power law decay in LdS and LAdS geometries instead of exponential suppression for the LM bulk.

In particular, Formulas (88) and (91) with $p = D-1$ describe the behavior of the current density for large values of $L_{(\mathrm{p})D}$ in models with a single compact dimension $x^D$. In that special case, the asymptotic of the Minkowskian current density for a massive field is described by (87). In order to display the essential difference of the large $L_{(\mathrm{p})r}$ asymptotics for LdS and LAdS from that in the LM geometry, in Figures 5 and 6, we present the ratios $\langle j^D\rangle/\langle j^D\rangle_{\mathrm{LM}}$ for $D = 4$ LdS and LAdS spacetimes; here, there is a single compact dimension of the proper length $L_{(\mathrm{p})} = L_{(\mathrm{p})D}$, as functions of $ma$ and $L_{(\mathrm{p})}/a$ for fixed $\tilde{\alpha}_D = 2\pi/5$. The ratios are evaluated for the same values of the proper lengths in the LM, LdS, and LAdS spacetimes and all the quantities are measured in units of $a$.

If at least one of the phases $\tilde{\alpha}_i$, $i \neq r$, is different from zero and the proper length $L_{(\mathrm{p})r}$ is large, we use the asymptotic expression of the Macdonald function for major discussions. For the LAdS geometry and LdS geometry with positive values of $\nu$, the leading contribution to the series over $n_r$ comes from the term $n_r = 1$, and we obtain

$$\langle j^r_{(\mathrm{p})}\rangle \approx \frac{2ea^{1+2\mu}B_D(am)\sin(\tilde{\alpha}_r)}{2^{\frac{p}{2}+\mu}\pi^{\frac{p}{2}}V_q^{(\mathrm{p})}L_{(\mathrm{p})r}^{p+1+2\mu}}(L_r|\mathbf{k}^{(0)}_{q-1}|)^{\frac{p}{2}+1+\mu}e^{-L_r|\mathbf{k}^{(0)}_{q-1}|}, \tag{93}$$

where, as before, $\mu = -\nu$ and $\mu = \nu_+$ for LdS and LAdS. In the case of LdS bulk and imaginary $\nu$, the leading order term takes the form

$$\left\langle j^r_{(\mathrm{p})}\right\rangle \approx \frac{4e\eta^{D+1}\sin(\tilde{\alpha}_r)}{(2\pi)^{\frac{p+1}{2}}a^DV_qL_r^{p+1}}\frac{(L_r|\mathbf{k}^{(0)}_{q-1}|)^{\frac{p}{2}+1}e^{-|\mathbf{k}^{(0)}_{q-1}|L_r}}{\sqrt{2|\nu|\sinh(\pi|\nu|)}}\cos\left[|\nu|\ln\left(|\mathbf{k}^{(0)}_{q-1}|\frac{L_r}{2}\right)-\arg(\Gamma(i|\nu|))\right]. \tag{94}$$

In the case of LdS, the different asymptotic behavior for positive and imaginary values of $\nu$ is related to different asymptotics of the function $[I_\nu(x)+I_{-\nu}(x)]K_\nu(x)$ for small arguments. For the LdS geometry and $\nu = 0$ for the leading contribution, we obtain

$$\left\langle j^r_{(\mathrm{p})} \right\rangle \approx \frac{4e\sin(\tilde{\alpha}_r)\eta^{D+1}}{(2\pi)^{\frac{p}{2}+1}a^D V_q L_r^{p+1}} (|\mathbf{k}^{(0)}_{q-1}|L_r)^{\frac{p}{2}+1} e^{-|\mathbf{k}^{(0)}_{q-1}|L_r} \ln\left(|\mathbf{k}^{(0)}_{q-1}|L_r\right). \tag{95}$$

Now, let us consider the asymptotics with respect to the length of the $l$th dimension with $l \neq r$. For large values $L_l$ compared with the other length scales and for $L_{(\mathrm{p})l}/a \gg 1$, the leading contribution to (68) comes from the term with $n_l = 0$. As expected, this leading term coincides with the current density in the geometry where the $l$th dimension is decompactified. The corrections induced by the respective compactification are suppressed by the factor $e^{-mL_l}$ ($1/L_l^{D+1}$ for a mass-less field) in the LM bulk and by the factor $1/L_l^{D+2+2\mu}$ for LdS and LAdS geometries, where $\mu$ is given by (89).

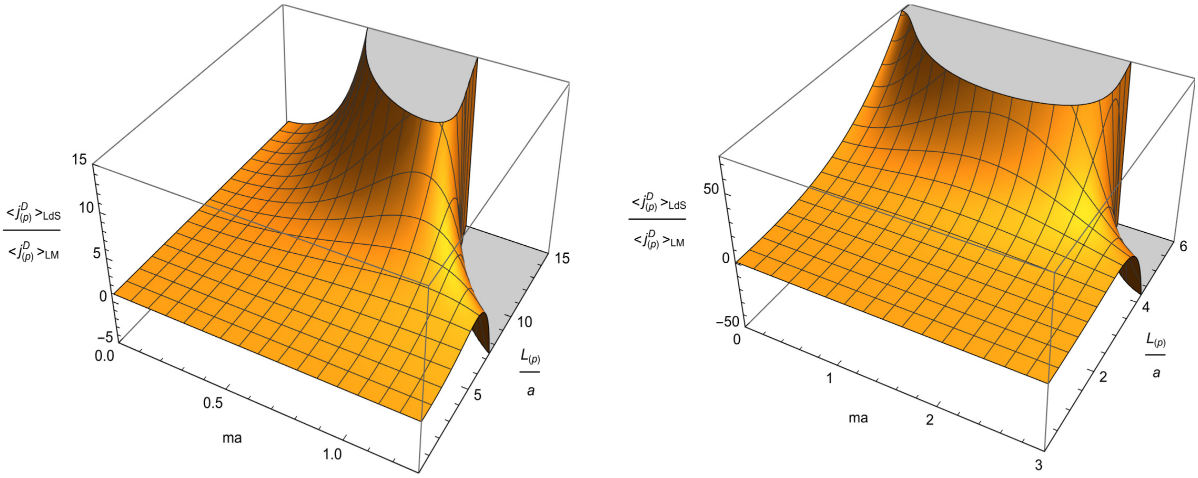


**Figure 5.** The ratio of the current densities in the $D = 4$ LdS and LM spacetimes with the same proper lengths of the single compact dimension versus the mass and the proper length (in units of $a$). The left and right panels correspond to conformally and minimally coupled fields; the graphs are plotted for $\tilde{\alpha}_D = 2\pi/5$.

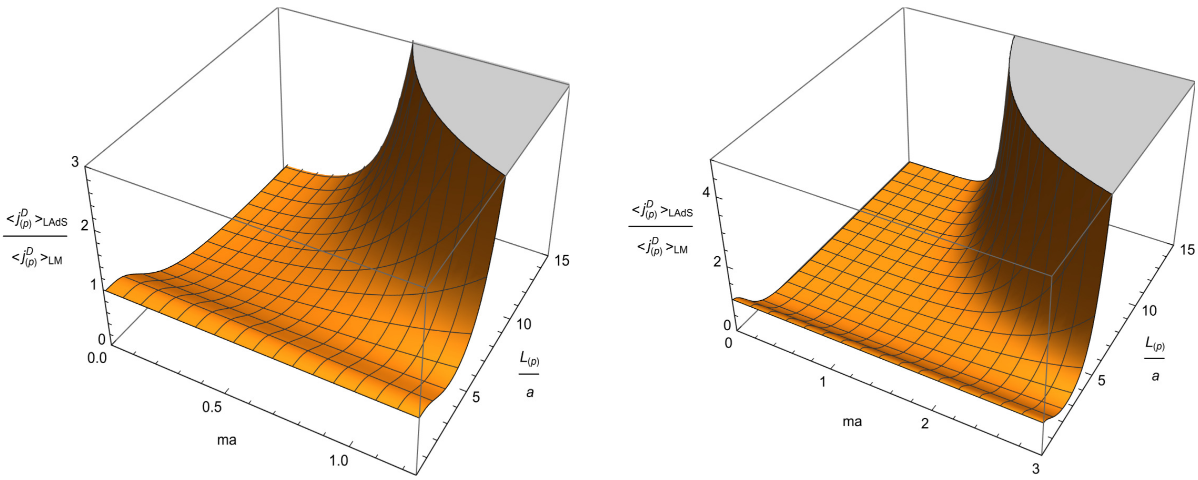


**Figure 6.** The same as in Figure 5 for the LAdS spacetime.

In the opposite limit of small values of $L_l$, it is more convenient to use the representations (22) and (72). The behavior of the current density is essentially different for the cases $\tilde{\alpha}_l = 0$ and $\tilde{\alpha}_l \neq 0$. In the first case, the dominant contribution to the summation over $\mathbf{n}_{q-1}$ comes from the modes with $n_l = 0$. For the LM bulk, the leading term in the expansion of $L_{(\mathrm{p})l}\left\langle j^r_{(\mathrm{p})}\right\rangle$ coincides with the current density in $D$-dimensional LM spacetime, which is obtained from the initial $(D+1)$-dimensional spacetime, excluding the $l$th dimension. The same is the case for the LdS and LAdS bulks with the difference that, in the leading terms of the expansion for $L_{(\mathrm{p})l}\left\langle j^r_{(\mathrm{p})}\right\rangle$, the parameters $\nu$ and $\nu_+$ are defined for $(D+1)$-dimensional spacetime; in contrast, in the formula for the $D$-dimensional current density $\left\langle j^r_{(\mathrm{p})}\right\rangle$, the corresponding expressions for $\nu$ and $\nu_+$ are obtained from (41) and (57) through the replacement $D \to D-1$. For small values of $L_l$ and $\tilde{\alpha}_l \neq 0$, the contribution of the modes with $n_r = 1$ and $n_l = 0$ dominates in (22) and (72). In the remaining summations over $n_i$, $i \neq r, l$, the main contribution comes from large values $n_i$ and we replace the corresponding series through integrations. In this way, it can be seen that the current density $\left\langle j^r_{(\mathrm{p})}\right\rangle$ is suppressed by the factor $\exp(-L_r|\tilde{\alpha}_l|/L_l)$.

### 6.4. Fermionic Currents

In the discussion above, we have considered the current densities for a charged scalar field. Similar investigations for the massive Dirac field $\psi(x)$ in general number of spatial dimensions, obeying the quasi-periodicity conditions

$$\psi(t, x^1, \ldots, x^p, \ldots, x^l + L_l, \ldots, x^D) = e^{i\alpha_l}\psi(t, x^1, \ldots, x^p, \ldots, x^l, \ldots, x^D), \tag{96}$$

with constant phases $\alpha_l$, are presented in [17,22,24] for LM, LdS, and LAdS geometries, respectively. The formulas from these references for the fermionic current density along the $r$th compact dimension are presented in the combined form

$$\left\langle j^r_{(\mathrm{p})}\right\rangle_{(\mathrm{f})} = -\frac{NeL_{(\mathrm{p})r}}{(2\pi)^{\frac{D+1}{2}}a^{D+1}}\sum_{\mathbf{n}_q} n_r \sin(\mathbf{n}_q \cdot \tilde{\boldsymbol{\alpha}}_q) F^{(\mathrm{f})}_D(am, g(\mathbf{L}_{(\mathrm{p})q}/a, \mathbf{n}_q)), \tag{97}$$

with the same notations as in (68). Here, $N = 2^{\left[\frac{D+1}{2}\right]}$ ($[x]$ stands for the integer part of $x$) is the number of spinor components for the Dirac field, realizing the irreducible representation of the Clifford algebra. The functions $F^{(\mathrm{f})}_D(am, x)$ in (97) are defined by

$$\begin{aligned} F^{(\mathrm{f})}_D(am, x) &= F_D(am, x), \text{ for LM}, \\ F^{(\mathrm{f})}_D(am, x) &= \frac{1}{2}\mathrm{Re}\left[p^{-\frac{D+1}{2}}_{i\alpha m}\left(x^2/2 - 1\right)\right], \text{ for LdS}, \\ F^{(\mathrm{f})}_D(am, x) &= \frac{1}{2}\left[q^{\frac{D+1}{2}}_{am}\left(x^2/2+1\right) + q^{\frac{D+1}{2}}_{am-1}\left(x^2/2+1\right)\right], \text{ for LAdS}. \end{aligned} \tag{98}$$

The replacement $2\pi\tilde{\alpha}_l \to -\tilde{\alpha}_l$ in the expression for LM bulk, compared to the one given in [17], is related to different notations of the constants in the quasi-periodicity conditions (see also the comment in [24]). The applications of (97), with $D = 2$, in cylindrical nanotubes, described in terms of the effective Dirac theory, have been discussed in [17,24].

As can be seen in (98), assuming the same masses and phases in the periodicity conditions for scalar and Dirac fields, the relation $\langle j^l\rangle_{(\mathrm{f})\mathrm{LM}} = -(N/2)\langle j^l\rangle_{\mathrm{LM}}$ is obtained for the corresponding current densities in LM bulk. In particular, in supersymmetric models with the same number of scalar and spinor degrees of freedom, the total vacuum current vanishes. That is not the case for the LdS and LAdS geometries. In an even number of spatial dimensions $D$, the Clifford algebra has two non-equivalent representations with two different sets of the Dirac matrices. As was discussed in [24], the vacuum current densities coincide for the fields, realizing those representations if the corresponding masses and the periodicity conditions are the same. More details of the properties for fermionic currents in LM, LdS, and LAdS geometries with toroidal compact dimensions will be reviewed elsewhere.

## 7. Conclusions

In the present paper, we have discussed the features of the vacuum currents in field–theoretical models formulated in the context of spacetimes with compact dimensions. Three cases of background geometries are considered: LM, LdS, and LAdS. In the decompactification limit, they correspond to maximally symmetric solutions of Einstein field equations in $(D+1)$-dimensional spacetime with zero, positive, and negative cosmological constants, respectively. The toroidal compactification of a part of spatial dimensions does not change the local geometrical characteristics; additionally, the high symmetry allowed us to find the closed analytic expressions for the vacuum currents along the compact dimensions. For an external gauge field, we have taken the simplest configuration with a constant gauge field. However, the corresponding magnetic field is zero; this is because the nontrivial topology respective vector potential gives rise to an Aharonov–Bohm-like effect on the vacuum characteristics. Through a gauge transformation, the gauge field potential is reinterpreted in terms of the phases in the periodicity conditions on the field operator along the compact dimensions. The quasi-periodicity conditions with nontrivial phases break the reflection symmetry in the respective directions; as a consequence, the contributions of the left- and right-moving modes of the vacuum fluctuations in the quantum field do not compensate for each other. As a result, a net current appears that is the analog of the persistent currents in the mesoscopic metallic rings.

The combined expression for the current density along the $r$th compact dimension, valid for all three background geometries, is given by the Formula (68). The information on specific geometry is encoded in the function $F_D(am, x)$, defined by (69). The component of the current density $\left\langle j^r_{(\mathrm{p})} \right\rangle$ is an odd periodic function of the phase $\tilde{\alpha}_r$ with the period $2\pi$ and an even periodic function of the remaining phases $\tilde{\alpha}_l$, $l \neq r$, with the same period. This periodicity is also interpreted as periodicity in terms of the magnetic flux enclosed by compact dimensions. In this interpretation, the period is equal to the flux quantum. For curved backgrounds, the current density depends on the lengths of the compact dimensions and on the coordinates (temporal $\tau$ and spatial $z$ coordinates for LdS and LAdS, respectively) in the form of the proper lengths $L_{(\mathrm{p})l}$. This feature is a consequence of the maximal symmetry of the dS and AdS spacetimes. For a conformally coupled mass-less scalar field, the current densities in the LM and LdS spacetimes are connected by the standard relation (75). For LAdS geometry, one has a conformal relation with the current density in LM spacetime (given by (76)), with an additions planar boundary that is perpendicular to one of the non-compact dimensions. The boundary in the LM spacetime with the Dirichlet boundary condition on the scalar field operator is the conformal image of the AdS boundary.

For LdS and LAdS bulks and for small values of the length of the compact dimension, the mode sum of the component of the current density along that dimension is dominated by the contribution of the vacuum fluctuations with wavelengths that are smaller than the curvature radius. The influence of the gravitational field on those modes is weak; the leading term in the respective expansion, given by (83), coincides with that for the LM bulk, with the length of the compact dimension replaced by the proper lengths for the LdS and LAdS geometries. The leading term presents the current density for a mass-less field in $(D+1)$-dimensional LM spacetime with a single compact dimension of the length $L_{(\mathrm{p})r}$. For small values of the length of the $l$th compact dimension, the behavior of the current density along the $r$th dimension, $r \neq l$, essentially differs for zero and nonzero values of the phase $|\tilde{\alpha}_l| \leq 1/2$. In the first case, $\tilde{\alpha}_l = 0$—the dominant contribution to the current density $\left\langle j^r_{(\mathrm{p})} \right\rangle$—comes from the zero mode $n_l = 0$ and the leading term in the expansion of the product $L_{(\mathrm{p})l} \left\langle j^r_{(\mathrm{p})} \right\rangle$ coincides with the corresponding current density in

$D$-dimensional spacetime with spatial coordinates $(x^1,\ldots,x^{l-1},x^{l+1},\ldots,x^D)$. For $\tilde{\alpha}_l \neq 0$, the zero mode with respect to the $l$th dimension is absent and the component $\left\langle j^r_{(\mathrm{p})} \right\rangle$ decays like $\exp(-|\tilde{\alpha}_l|L_r/L_l)$.

The effect of the spacetime curvature on the current density is essential for lengths of compact dimensions of the order or larger compared with the curvature radius. For large values of the length of the $r$th compact dimension, the asymptotic of the current $\left\langle j^r_{(\mathrm{p})} \right\rangle$ is completely different for the cases $\omega_{0r}=0$ and $\omega_{0r}\neq 0$ with $\omega_{0r}=\sqrt{k^{(0)2}_{\mathbf{n}_{q-1}}+m^2}$ and $k^{(0)2}_{\mathbf{n}_{q-1}}$, defined by (84). For $\omega_{0r}=0$, corresponding to a mass-less field with zero phases $\tilde{\alpha}_l$, $l\neq r$, the leading term for the LM bulk is given by (85). Multiplied by $V_q/L_r$, that expression gives the current density for a mass-less field in $(p+2)$-dimensional LM spacetime with a single compact dimension $x^r$. For $\omega_{0r}\neq 0$, the large $L_r$ asymptotic is described by (86) and the current density in the LM bulk is exponentially suppressed. For the LdS and LAdS background geometries and for $\tilde{\alpha}_l=0$, $l\neq r$, the leading term in the large $L_{(\mathrm{p})r}$ asymptotic is given by the right-hand side of (88), with $\nu>0$ for the LdS bulk. This shows that the gravitational field essentially changes the behavior of the current density for large lengths of compact dimensions: instead of the exponential suppression in the LM bulk for a massive field, for the LdS and LAdS geometries, the fall-off of the current density follows a power law. For the LdS background and for imaginary values of the parameter $\nu$, the behavior of the current density is described by (94). In this case, the decay with respect to $L_r$ is oscillatory, with the amplitude decreasing as $1/L_r^{p+1}$. In the case when at least one of the phases $\tilde{\alpha}_l=0$, $l\neq r$, differs from zero, the asymptotic behavior of the current density $\left\langle j^r_{(\mathrm{p})} \right\rangle$ is given by (93) for LAdS and for LdS in the range $\nu>0$ with an exponential decay. For LdS bulk and imaginary $\nu$, the decay is oscillatory (see (94)).

The current density along compact dimensions is a source of magnetic fields that has components in the non-compact sub-space. In spatial dimensions $D>3$, the magnetic field is a spatial tensor of rank $D-2$, which can be found by solving Maxwell's $(D+1)$-dimensional semi-classical equations with the VEV of the current density as a source. That would be an interesting application of the results described in the present paper. Note that several mechanisms for the generation of the seeds for cosmological magnetic fields in higher-dimensional models have been discussed in the literature (see, for example, [102,103]).

**Funding:** This research was supported by the grant No. 21AG-1C047 of the Higher Education and Science Committee of the Ministry of Education, Science, Culture and Sport RA and by the ANSEF grant 23AN:PS-hepth-2889.

**Data Availability Statement:** Data are contained in the article.

**Acknowledgments:** I am grateful to Stefano Bellucci, Eugenio Ramos Bezerra de Mello, and Valeri Vardanyan for their fruitful collaboration.

**Conflicts of Interest:** The author declares no conflict of interest.

## Appendix A. Properties of the Functions in the Expressions for the Currents

We have seen that the vacuum currents along compact dimensions in LdS and LAdS geometries are expressed in terms of the functions (51) and (64). Here, the properties of those functions are considered. First of all, we note that they are expressed in terms of the hypergeometric function as

$$
\begin{aligned}
p^{-\mu}_{\nu-\frac{1}{2}}(u) &= \frac{\Gamma(\mu+\frac{1}{2}-\nu)\Gamma(\mu+\frac{1}{2}+\nu)}{2^{\mu}\Gamma(\mu+1)}F\left(\mu+\frac{1}{2}-\nu,\mu+\frac{1}{2}+\nu;\mu+1;\frac{1-u}{2}\right),\\
q^{\mu}_{\nu-\frac{1}{2}}(u) &= \frac{\sqrt{\pi}\Gamma(\mu+\nu+\frac{1}{2})}{2^{\nu+\frac{1}{2}}\Gamma(\nu+1)u^{\mu+\nu+\frac{1}{2}}}F\left(\frac{\mu+\nu+\frac{3}{2}}{2},\frac{\mu+\nu+\frac{1}{2}}{2};\nu+1;\frac{1}{u^2}\right).
\end{aligned}
\tag{A1}
$$

By using the recurrence relations for the associated Legendre functions, one can see that $\partial_u p_\alpha^{-\mu}(u) = -p_\alpha^{-\mu-1}(u)$ and $\partial_u q_\alpha^{\mu}(u) = -q_\alpha^{\mu+1}(u)$. From here, we obtain the relations

$$p_\alpha^{-\mu-n}(u) = (-1)^n \partial_u^n p_\alpha^{-\mu}(u),\ q_\alpha^{\mu+n}(u) = (-1)^n \partial_u^n q_\alpha^{\mu}(u), \tag{A2}$$

with $n = 1, 2, \ldots$.

In the physical problems under consideration, depending on the spatial dimension, the order $\mu$ for the functions $p_\alpha^{-\mu}(u)$ and $q_\alpha^{\mu}(u)$ is a positive integer or half-integer. By making use of (A2), these functions are expressed in terms of $p_\alpha^0(u)$ and $q_\alpha^0(u)$ or $p_\alpha^{-1/2}(u)$ and $q_\alpha^{1/2}(u)$. Employing the corresponding expressions for the functions $P_\alpha^{-1/2}(u)$ and $Q_\alpha^{1/2}(u)$ from [81], one obtains

$$\begin{aligned}
p_{\nu-1/2}^{-1/2}(\cosh\zeta) &= \frac{\sqrt{2\pi}\sinh(\nu\zeta)}{\sin(\pi\nu)\sinh\zeta}, \\
p_{\nu-1/2}^{-1/2}(\cos\theta) &= \frac{\sqrt{2\pi}\sin(\nu\theta)}{\sin(\pi\nu)\sin\theta}, \\
q_{\nu-1/2}^{1/2}(\cosh\zeta) &= \sqrt{\frac{\pi}{2}}\frac{e^{-\nu\zeta}}{\sinh\zeta}.
\end{aligned} \tag{A3}$$

Combining these expressions with the relations (A2) for even values of the spatial dimension $D$, we obtain

$$F_D(am, x) = \sqrt{\frac{\pi}{2}}(-1)^{\frac{D}{2}}\left(\frac{\partial_\xi}{\sinh\xi}\right)^{\frac{D}{2}}\frac{e^{-\nu_+\xi}}{\sinh\xi},\ x = 2\sinh(\xi/2), \tag{A4}$$

in LAdS geometry and

$$\begin{aligned}
F_D(am, x) &= \frac{(-1)^{\frac{D}{2}}\sqrt{\pi/2}}{\sin(\pi\nu)}\left(\frac{\partial_\xi}{\sinh\xi}\right)^{\frac{D}{2}}\frac{\sinh(\nu\xi)}{\sinh\xi},\ x = 2\cosh(\xi/2), \\
F_D(am, x) &= \frac{\sqrt{\pi/2}}{\sin(\pi\nu)}\left(\frac{\partial_\theta}{\sin\theta}\right)^{\frac{D}{2}}\frac{\sin(\nu\theta)}{\sin\theta},\ x = 2\cos(\theta/2),
\end{aligned} \tag{A5}$$

for LdS bulk. For odd values of $D$, one has

$$\begin{aligned}
F_D(am, x) &= \frac{1}{2}(-1)^{\frac{D+1}{2}}\Gamma\left(\frac{1}{2}-\nu\right)\Gamma\left(\nu+\frac{1}{2}\right)\partial_u^{\frac{D+1}{2}}P_{\nu-\frac{1}{2}}(u),\ \text{for LdS}, \\
F_D(am, x) &= (-1)^{\frac{D+1}{2}}\partial_u^{\frac{D+1}{2}}Q_{\nu_+-\frac{1}{2}}(u),\ \text{for LAdS},
\end{aligned} \tag{A6}$$

where $u = x^2/2 - 1$ for LdS and $u = x^2/2 + 1$ for LAdS.

In order to find the behavior of the functions $p_{\nu-1/2}^{-\mu}(u)$ and $q_{\nu-1/2}^{\mu}(u)$ for large values of $u$, we use the corresponding asymptotics for the associated Legendre functions (see, for example, [99]). The leading order terms read

$$\begin{aligned}
p_{\nu-\frac{1}{2}}^{-\mu}(u) &\sim \frac{2^{\nu-\frac{1}{2}}}{\sqrt{\pi}}\frac{\Gamma(\nu)\Gamma\left(\mu+\frac{1}{2}-\nu\right)}{u^{\mu-\nu+\frac{1}{2}}},\ \mathrm{Re}\,\nu > 0,\ \mu+\nu \neq -1, -2, \ldots, \\
p_{-\frac{1}{2}}^{-\mu}(u) &\sim \sqrt{\frac{2}{\pi}}\Gamma\left(\mu+\frac{1}{2}\right)\frac{\ln u}{u^{\mu+\frac{1}{2}}},\ \mu \neq -\frac{1}{2}, -\frac{3}{2}, \ldots, \\
q_{\nu-\frac{1}{2}}^{\mu}(u) &\sim \frac{\sqrt{\pi}\Gamma\left(\mu+\nu+\frac{1}{2}\right)}{2^{\nu+\frac{1}{2}}\Gamma(\nu+1)u^{\mu+\nu+\frac{1}{2}}},\ \nu \neq -\frac{3}{2}, -\frac{5}{2}, \ldots
\end{aligned} \tag{A7}$$

The asymptotic for $p^{-\mu}_{\nu-\frac{1}{2}}(u)$ in the case of purely imaginary values of $\nu$, $\nu = i|\nu|$, is obtained using the relation [99]

$$P^{-\mu}_{i|\nu|-\frac{1}{2}}(u) = ie^{-i\mu\pi i}\frac{Q^{\mu}_{i|\nu|-\frac{1}{2}}(u) - Q^{\mu}_{-i|\nu|-\frac{1}{2}}(u)}{\sinh(|\nu|\pi)|\Gamma\left(\mu+\frac{1}{2}+i|\nu|\right)|^2}, \quad (A8)$$

and the corresponding asymptotic for $Q^{\mu}_{i|\nu|-\frac{1}{2}}(u)$. This gives

$$p^{-\mu}_{i|\nu|-\frac{1}{2}}(u) \sim \frac{\sqrt{2/\pi}}{u^{\mu+\frac{1}{2}}}\,\mathrm{Re}\left[\Gamma\left(\mu+\frac{1}{2}-i|\nu|\right)\frac{\Gamma(i|\nu|)}{(2u)^{i|\nu|}}\right]. \quad (A9)$$

These asymptotic formulas have been used in the main text to study the behavior of the current density in asymptotic regions of the parameters.

## References

1. Ford, L.H.; Yoshimura, T. Mass generation by self-interaction in non-Minkowskian spacetimes. *Phys. Lett. A* **1979**, *70*, 89–91. [CrossRef]
2. Scherk, J.; Schwarz, J.H. How to get masses from extra dimensions. *Nucl. Phys. B* **1979**, *153*, 61–68. [CrossRef]
3. Ford, L.H. Instabilities in interacting quantum field theories in non-Minkowskian spacetimes. *Phys. Rev. D* **1980**, *22*, 3003–3011. [CrossRef]
4. Toms, D.J. Casimir effect and topological mass. *Phys. Rev. D* **1980**, *21*, 928–932. [CrossRef]
5. Toms, D.J. Symmetry breaking and mass generation by space-time topology. *Phys. Rev. D* **1980**, *21*, 2805–2817. [CrossRef]
6. Odintsov, S.D. Effective action in multidimensional gauged supergravities and spontaneous compactification. *Sov. J. Nucl. Phys.* **1988**, *48*, 729–733.
7. Hosotani, Y. Dynamics of non-integrable phases and gauge symmetry breaking. *Ann. Phys.* **1989**, *190*, 233–253. [CrossRef]
8. Buchbinder, I.L.; Odintsov, S.D. Spontaneous supersymmetry breaking and effective action in supersymmetrical Kaluza-Klein theories and strings. *Int. J. Mod. Phys. A* **1989**, *4*, 4337–4351. [CrossRef]
9. Quiros, M. New ideas in symmetry breaking. *arXiv* **2003**, arXiv:hep-ph/0302189.
10. Mostepanenko, V.M.; Trunov, N.N. *The Casimir Effect and Its Applications*; Clarendon Press: Oxford, NY, USA, 1997.
11. Milton, K.A. *The Casimir Effect: Physical Manifestation of Zero-Point Energy*; World Scientific: Singapore, 2002.
12. Bordag, M.; Klimchitskaya, G.L.; Mohideen, U.; Mostepanenko, V.M. *Advances in the Casimir Effect*; Oxford University Press: New York, NY, USA, 2009.
13. Milonni, P.; Roberts, D.; da Rosa, F. Lecture Notes in Physics. In *Casimir Physics*; Dalvit, D., Ed.; Springer: Berlin, Germany, 2011; Volume 834.
14. Elizalde, E.; Odintsov, S.D.; Romeo, A.; Bytsenko, A.A.; Zerbini, S. *Zeta Regularization Techniques with Applications*; World Scientific: Singapore, 1994.
15. Candelas, P.; Weinberg, S. Calculation of gauge couplings and compact circumferences from self-consistent dimensional reduction. *Nucl. Phys. B* **1984**, *237*, 397–441. [CrossRef]
16. Bezerra de Mello, E.R.; Saharian, A.A. Finite temperature current densities and Bose–Einstein condensation in topologically nontrivial spaces. *Phys. Rev. D* **2013**, *87*, 045015. [CrossRef]
17. Bellucci, S.; Saharian, A.A.; Bardeghyan, V.M. Induced fermionic current in toroidally compactified spacetimes with applications to cylindrical and toroidal nanotubes. *Phys. Rev. D* **2010**, *82*, 065011. [CrossRef]
18. Gusynin, V.P.; Sharapov, S.G.; Carbotte, J.P. AC conductivity of graphene: From tight-binding model to 2+1-dimensional quantum electrodynamics. *Int. J. Mod. Phys. B* **2007**, *21*, 4611–4658. [CrossRef]
19. Castro Neto, A.H.; Guinea, F.; Peres, N.M.R.; Novoselov, K.S.; Geim, A.K. The electronic properties of graphene. *Rev. Mod. Phys.* **2009**, *81*, 109–162. [CrossRef]
20. Bellucci, S.; Saharian, A.A.; Saharyan, N.A. Casimir effect for scalar current densities in topologically nontrivial spaces. *Eur. Phys. J. C* **2015**, *75*, 378. [CrossRef]
21. Bellucci, S.; Saharian, A.A. Fermionic current from topology and boundaries with applications to higher-dimensional models and nanophysics. *Phys. Rev. D* **2013**, *87*, 025005. [CrossRef]
22. Bellucci, S.; Saharian, A.A.; Nersisyan, H.A. Scalar and fermionic vacuum currents in de Sitter spacetime with compact dimensions. *Phys. Rev. D* **2013**, *88*, 024028. [CrossRef]
23. Bezerra de Mello, E.R.; Saharian, A.A.; Vardanyan, V. Induced vacuum currents in anti-de Sitter space with toral dimensions. *Phys. Lett. B* **2015**, *741*, 155–162. [CrossRef]
24. Bellucci, S.; Saharian, A.A.; Vardanyan, V. Fermionic currents in AdS spacetime with compact dimensions. *Phys. Rev. D* **2017**, *96*, 065025. [CrossRef]

25. Bellucci, S.; Saharian, A.A.; Vardanyan, V. Vacuum currents in braneworlds on AdS bulk with compact dimensions. *JHEP* **2015**, *11*, 092. [CrossRef]
26. Bellucci, S.; Saharian, A.A.; Vardanyan, V. Hadamard function and the vacuum currents in braneworlds with compact dimensions: Two-branes geometry. *Phys. Rev. D* **2016**, *93*, 084011. [CrossRef]
27. Bellucci, S.; Saharian, A.A.; Simonyan, D.H.; Vardanyan, V.V. Fermionic currents in topologically nontrivial braneworlds. *Phys. Rev. D* **2018**, *98*, 085020. [CrossRef]
28. Bellucci, S.; Saharian, A.A.; Sargsyan, H.G.; Vardanyan, V.V. Fermionic vacuum currents in topologically nontrivial braneworlds: Two-brane geometry. *Phys. Rev. D* **2020**, *101*, 045020. [CrossRef]
29. Büttiker, M.; Imry, Y.; Landauer, R. Josephson behavior in small normal one-dimensional rings. *Phys. Lett. A* **1983**, *96*, 365–367. [CrossRef]
30. Cheung, H.-F.; Gefen, Y.; Riedel, E.K.; Shih, W.-H. Persistent currents in small one-dimensional metal rings. *Phys. Rev. B* **1988**, *37*, 6050–6062. [CrossRef]
31. Cheung, H.-F.; Riedel, E.K.; Gefen, Y. Persistent currents in mesoscopic rings and cylinders. *Phys. Rev. Lett.* **1989**, *62*, 587–590. [CrossRef] [PubMed]
32. Altshuler, B.L.; Gefen, Y.; Imry, Y. Persistent differences between canonical and grand canonical averages in mesoscopic ensembles: Large paramagnetic orbital susceptibilities. *Phys. Rev. Lett.* **1991**, *66*, 88–91. [CrossRef] [PubMed]
33. von Oppen, F.; Riedel, E.K. Average persistent current in a mesoscopic ring. *Phys. Rev. Lett.* **1991**, *66*, 84–87. [CrossRef]
34. Abraham, M.; Berkovits, R. Persistent currents in an interacting 1D disordered ring: Manifestations of the Mott-Hubbard transition. *Phys. Rev. Lett.* **1993**, *70*, 1509–1512. [CrossRef]
35. Recher, P.; Trauzettel, B.; Rycerz, A.; Blanter, Y.M.; Beenakker, C.W.J.; Morpurgo, A.F. Aharonov–Bohm effect and broken valley degeneracy in graphene rings. *Phys. Rev. B* **2007**, *76*, 235404. [CrossRef]
36. Imry, Y. *Introduction to Mesoscopic Physics*; Oxford University Press: New York, NY, USA, 2008.
37. Akkermans, E.; Montambaux, G. *Mesoscopic Physics of Electrons and Photons*; Cambridge University Press: Cambridge, UK, 2011.
38. Michetti, P.; Recher, P. Bound states and persistent currents in topological insulator rings. *Phys. Rev. B* **2011**, *83*, 125420. [CrossRef]
39. Huang, B.-L.; Chang, M.-C.; Mou, C.-Y. Persistent currents in a graphene ring with armchair edges. *J. Phys. Condens. Matter* **2012**, *24*, 245304. [CrossRef] [PubMed]
40. Sticlet, D.; Dóra, B.; Cayssol, J. Persistent currents in Dirac fermion rings. *Phys. Rev. B* **2013**, *88*, 205401. [CrossRef]
41. Ghosh, S.; Saha, A. Persistent current of relativistic electrons on a Dirac ring in presence of impurities. *Eur. Phys. J. B* **2014**, *87*, 167. [CrossRef]
42. Bolivar, N.; Medina, E.; Berche, B. Persistent charge and spin currents in the long-wavelength regime for graphene rings. *Phys. Rev. B* **2014**, *89*, 125413. [CrossRef]
43. Ying, L.; Lai, Y.-C. Robustness of persistent currents in two-dimensional Dirac systems with disorder. *Phys. Rev. B* **2017**, *96*, 165407. [CrossRef]
44. Amico, L.; Birkl, G.; Boshier, M.; Kwek, L.-C. Focus on atomtronics-enabled quantum technologies. *New J. Phys.* **2017**, *19*, 020201. [CrossRef]
45. Fomin, V.M. (Ed.) *Physics of Quantum Rings*; Springer International Publishing: Cham, Switzerland, 2018.
46. Jurkowski, P.; Szafran, B. Persistent currents in topological and trivial confinement in silicene. *Phys. Rev. B* **2020**, *101*, 075408. [CrossRef]
47. Yerin, Y.; Gusynin, V.P.; Sharapov, S.G.; Varlamov, A.A. Genesis and fading away of persistent currents in a Corbino disk geometry. *Phys. Rev. B* **2021**, *104*, 075415. [CrossRef]
48. Tengstrand, M.N.; Boholm, D.; Sachdeva, R.; Bengtsson, J.; Reimann, S.M. Persistent currents in toroidal dipolar supersolids. *Phys. Rev. B* **2021**, *103*, 013313. [CrossRef]
49. Amico, L.; Anderson, D.; Boshier, M.; Brantut, J.-P.; Kwek, L.-C.; Minguzzi, A.; von Klitzing, W. Colloquium: Atomtronic circuits: From many-body physics to quantum technologies. *Rev. Mod. Phys.* **2022**, *94*, 041001. [CrossRef]
50. Chetcuti, W.J.; Haug, T.; Kwek, L.-C.; Amico, L. Persistent current of SU(N) fermions. *SciPost Phys.* **2022**, *12*, 033. [CrossRef]
51. Lévy, L.P.; Dolan, G.; Dunsmuir, J.; Bouchiat, H. Magnetization of mesoscopic copper rings: Evidence for persistent currents. *Phys. Rev. Lett.* **1990**, *64*, 2074. [CrossRef] [PubMed]
52. Chandrasekhar, V.; Webb, R.A.; Brady, M.J.; Ketchen, M.B.; Gallagher, W.J.; Kleinsasser, A. Magnetic response of a single, isolated gold loop. *Phys. Rev. Lett.* **1991**, *67*, 3578–3581. [CrossRef] [PubMed]
53. Mailly, D.; Chapelier, C.; Benoit, A. Experimental observation of persistent currents in a GaAs-AlGaAs single loop. *Phys. Rev. Lett.* **1993**, *70*, 2020–2023. [CrossRef] [PubMed]
54. Kleemans, N.A.J.M.; Bominaar-Silkens, I.M.A.; Fomin, V.M.; Gladilin, V.N.; Granados, D.; Taboada, A.G.; García, J.M.; Offermans, P.; Zeitler, U.; Christianen, P.C.M.; et al. Oscillatory persistent currents in self-assembled quantum rings. *Phys. Rev. Lett.* **2007**, *99*, 146808. [CrossRef] [PubMed]
55. Bleszynski-Jayich, A.C.; Shanks, W.E.; Peaudecerf, B.; Ginossar, E.; von Oppen, F.; Glazman, L.; Harris, J.G.E. Persistent currents in normal metal rings. *Science* **2009**, *326*, 272. [CrossRef]
56. Bluhm, H.; Koshnick, N.C.; Bert, J.A.; Huber, M.E.; Moler, K.A. Persistent currents in normal metal rings. *Phys. Rev. Lett.* **2009**, *102*, 136802. [CrossRef]

57. Souche, G.M.; Huillery, J.; Pothier, H.; Gandit, P.; Mars, J.I.; Skipetrov, S.E.; Bourgeois, O. Searching for thermal signatures of persistent currents in normal-metal rings. *Phys. Rev. B* **2013**, *87*, 115120. [CrossRef]
58. Cai, Y.; Allman, D.G.; Sabharwal, P.; Wright, K.C. Persistent currents in rings of ultracold fermionic atoms. *Phys. Rev. Lett.* **2022**, *128*, 150401. [CrossRef]
59. Pace, G.D.; Xhani, K.; Falconi, A.M.; Fedrizzi, M.; Grani, N.; Rajkov, D.H.; Inguscio, M.; Scazza, F.; Kwon, W.J.; Roati, G. Imprinting persistent currents in tunable fermionic rings. *Phys. Rev. X* **2022**, *12*, 041037.
60. Hooft, G.T. A property of electric and magnetic flux in non-Abelian gauge theories. *Nucl. Phys.* **1979**, *B153*, 141–160. [CrossRef]
61. González-Arroyo, A. Yang–Mills fields on the 4-dimensional torus. Part I: Classical theory. *arXiv* **1998**, arXiv:hep-th/9807108.
62. Anber, M.M.; Poppitz, E. Nonperturbative effects in the Standard Model with gauged 1-form symmetry. *JHEP* **2021**, 12, 055. [CrossRef]
63. Elizalde, E. Spectrum of the Casimir effect on a torus. *Z. Phys. C* **1989**, *44*, 471–478. [CrossRef]
64. Tanaka, T.; Hiscock, W.A. Massive scalar field in multiply connected flat spacetimes. *Phys. Rev. D* **1995**, *52*, 4503–4511. [CrossRef]
65. Kleinert, H.; Zhuk, A. The Casimir effect at nonzero temperatures in a Universe with topology $S^1 \times S^1 \times S^1$. *Theor. Math. Phys.* **1996**, *108*, 1236–1248. [CrossRef]
66. Hofmann, R.; Kanti, P.; Pospelov, M. (De)stabilization of an extra dimension due to a Casimir force. *Phys. Rev. D* **2001**, *63*, 124020. [CrossRef]
67. Ahmadi, N.; Nouri-Zonoz, M. Massive spinor fields in flat spacetimes with nontrivial topology. *Phys. Rev. D* **2005**, *71*, 104012. [CrossRef]
68. Elizalde, E. Uses of zeta regularization in QFT with boundary conditions: A cosmo-topological Casimir effect. *J. Phys. A* **2006**, *39*, 6299–6307. [CrossRef]
69. Elizalde, E.; Odintsov, S.D.; Saharian, A.A. Repulsive Casimir effect from extra dimensions and Robin boundary conditions: From branes to pistons. *Phys. Rev. D* **2009**, *79*, 065023. [CrossRef]
70. Bellucci, S.; Saharian, A.A. Fermionic Casimir densities in toroidally compactified spacetimes with applications to nanotubes. *Phys. Rev. D* **2009**, *79*, 085019. [CrossRef]
71. Asorey M.; Cavero-Peláez, I.; Muñoz-Castañeda, M. Vacuum Energy and the Topology of the Universe. In *Cosmology, Quantum Vacuum and Zeta Functions*; Odintsov, S.D., Sáez-Gómes, D., Xambó-Descamps, S., Eds.; Springer: Berlin, Germany, 2011; pp. 35–44.
72. Oikonomou, V.K. Shape of compact toroidal dimensions $T_\theta^d$ and Casimir effect on $M \times T_\theta^d$ spacetime. *Commun. Theor. Phys.* **2011**, *55*, 101–110. [CrossRef]
73. Fornal, B.; Wise, M.B. Standard model with compactified spatial dimensions. *JHEP* **2011**, *7*, 086. [CrossRef]
74. Abreu, L.M.; Linhares, C.A.; Malbouisson, A.P.C.; Malbouisson, J.M.C. Magnetic effects on spontaneous symmetry breaking/restoration in a toroidal topology. *Phys. Rev. D* **2013**, *88*, 107701. [CrossRef]
75. Cao, C.J.; van Caspel, M.; Zhitnitsky, A.R. Topological Casimir effect in Maxwell electrodynamics on a compact manifold. *Phys. Rev. D* **2013**, *87*, 105012. [CrossRef]
76. Khanna, F.C.; Malbouisson, A.P.C.; Malbouisson, J.M.C.; Santana, A.E. Quantum field theory on toroidal topology: Algebraic structure and applications. *Phys. Rep.* **2014**, *539*, 135–224. [CrossRef]
77. Moreira, R.P.M.; Petronilo, G.X.A.; Santana, A.E.; Amorim, R.G.G.; Belich, H. CPT-even electrodynamics in a multidimensional torus: Casimir effect at finite temperature. *Eur. Phys. J. C* **2022**, *82*, 999. [CrossRef]
78. Haridev, S.R.; Samantray, P. Revisiting vacuum energy in compact spacetimes. *Phys. Lett. B* **2022**, *835*, 137489. [CrossRef]
79. Bellucci, S.; Bezerra de Mello, E.R.; Saharian, A.A. Finite temperature fermionic condensate and currents in topologically nontrivial spaces. *Phys. Rev. D* **2014**, *89*, 085002. [CrossRef]
80. Bezerra de Mello, E.R.; Saharian, A.A. Fermionic vacuum polarization by a composite topological defect in higher-dimensional space-time. *Phys. Rev. D* **2008**, *78*, 045021. [CrossRef]
81. Abramowitz, M.; Stegun, I.A. (Eds.) *Handbook of Mathematical Functions*; Dover: New York, NY, USA, 1972.
82. Kirsten, K. *Spectral Functions in Mathematics and Physics*; Chapman and Hall/CRC: Boca Raton, FL, USA, 2002.
83. Elizalde, E. *Ten Physical Applications of Spectral Zeta Functions*; Springer: Berlin/Heidelberg, Germany, 2012.
84. Elizalde, E. Multidimensional extension of the generalized Chowla-Selberg formula. *Commun. Math. Phys.* **1998**, *198*, 83–95. [CrossRef]
85. Griffiths, J.B.; Podolský, J. *Exact Space-Times in Einstein's General Relativity*; Cambridge University Press: Cambridge, UK, 2009.
86. Bunch, T.S.; Davies, P.C.W. Quantum field theory in de Sitter space: Renormalization by point-splitting. *Proc. R. Soc. Lond. Ser. A* **1978**, *360*, 117–134.
87. Prudnikov, A.P.; Brychkov, Y.A.; Marichev, O.I. *Integrals and Series*; Gordon and Breach: New York, NY, USA, 1986; Volume 2.
88. Aharony, O.; Gubser, S.S.; Maldacena, J.; Ooguri, H.; Oz, Y. Large N field theories, string theory and gravity. *Phys. Rep.* **2000**, *323*, 183–386. [CrossRef]
89. Năstase, H. *Introduction to AdS/CFT Correspondence*; Cambridge University Press: Cambridge, UK, 2015.
90. Ammon, M.; Erdmenger, J. *Gauge/Gravity Duality: Foundations and Applications*; Cambridge University Press: Cambridge, UK, 2015.
91. Natsuume, M. *AdS/CFT Duality User Guide*; Lecture Notes in Physics; Springer: Tokyo, Japan, 2015; Volume 903.
92. Maartens, R.; Koyama, K. Brane-world gravity. *Living Rev. Relativ.* **2010**, *13*, 5. [CrossRef]

93. Breitenlohner, P.; Freedman, D.Z. Positive energy in anti-de Sitter backgrounds and gauged extended supergravity. *Phys. Lett. B* **1982**, *115*, 197–201. [CrossRef]
94. Breitenlohner, P.; Freedman, D.Z. Stability in gauged extended supergravity. *Ann. Phys.* **1982**, *144*, 249–281. [CrossRef]
95. Mezincescu, L.; Townsend, P.K. Stability at a local maximum in higher dimensional anti-de Sitter space and applications to supergravity. *Ann. Phys.* **1985**, *160*, 406–419. [CrossRef]
96. Ishibashi, A.; Wald, R.M. Dynamics in non-globally-hyperbolic static spacetimes: II. General analysis of prescriptions for dynamics. *Class. Quantum Gravity* **2003**, *20*, 3815–3826. [CrossRef]
97. Ishibashi, A.; Wald, R.M. Dynamics in non-globally-hyperbolic static spacetimes: III. Anti-de Sitter spacetime. *Class. Quantum Gravity* **2004**, *21*, 2981–3013. [CrossRef]
98. Gradshteyn, I.S.; Ryzhik, I.M. *Table of Integrals, Series, and Products*; Elsevier: Amsterdam, The Netherlands, 2017.
99. Olver, F.W. *NIST Handbook of Mathematical Functions*; Cambridge University Press: New York, NY, USA, 2010.
100. Dunster, T.M. Bessel functions of purely imaginary order, with an application to second-order linear differential equations having a large parameter. *SIAM J. Math. Anal.* **1990**, *21*, 995–1018. [CrossRef]
101. Milton, K.A.; Wagner, J.; Kirsten, K. Casimir effect for a semitransparent wedge and an annular piston. *Phys. Rev. D* **2009**, *80*, 125028. [CrossRef]
102. Kandus, A.; Kunze, K.E.; Tsagas, C.G. Primordial magnetogenesis. *Phys. Rep.* **2011**, *505*, 1–58. [CrossRef]
103. Campanelli, L. Origin of cosmic magnetic fields. *Phys. Rev. Lett.* **2013**, *111*, 061301. [CrossRef]